Investigating the Neuroprotective Effects of Chenodeoxycholic Acid in MPTP-induced Parkinson's disease in BALB/c mice

By

Mehwish Mehreen

(Registration No: 00000401125)

Department of Biomedical engineering and Sciences

School of Mechanical and Manufacturing Engineering

National University of Sciences & Technology (NUST)

Islamabad, Pakistan

(2024)

Investigating the Neuroprotective Effects of Chenodeoxycholic Acid in MPTP-induced Parkinson's disease in BALB/c mice

By

Mehwish Mehreen

(Registration No: 00000401125)

A thesis submitted to the National University of Sciences and Technology, Islamabad,

in partial fulfillment of the requirements for the degree of

Master of Science in
Biomedical Sciences

Supervisor: Dr. Aneeqa Noor

School of Mechanical and Manufacturing Engineering

National University of Sciences & Technology (NUST)

Islamabad, Pakistan

(2024)

THESIS ACCEPTANCE CERTIFICATE

Certified that final copy of MS/MPhil thesis written by **Regn No. 00000401125 Mehwish Mehreen** of **School of Mechanical & Manufacturing Engineering (SMME)** has been vetted by undersigned, found complete in all respects as per NUST Statues/Regulations, is free of plagiarism, errors, and mistakes and is accepted as partial fulfillment for award of MS/MPhil degree. It is further certified that necessary amendments as pointed out by GEC members of the scholar have also been incorporated in the said thesis titled. **"Investigating the Effects of Chenodeoxycholic Acid in MPTP-Induced Parkinson's Disease Mouse Models."**

Signature:

Name (Supervisor): Aneeqa Noor

Date: 21 - Aug - 2024

Signature (HOD):

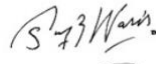**Date:** 21 - Aug - 2024

Signature (DEAN):

Date: 21 - Aug - 2024

National University of Sciences & Technology (NUST)
MASTER'S THESIS WORK

We hereby recommend that the dissertation prepared under our supervision by: Mehwish Mehreen (00000401125)
Titled: "Investigating the Effects of Chenodeoxycholic Acid in MPTP-Induced Parkinson's Disease Mouse Models." be accepted
in partial fulfillment of the requirements for the award of MS in Biomedical Sciences degree.

Examination Committee Members

1. Name: Muhammad Asim Waris   Signature:

2. Name: Adeeb Shehzad   Signature:

Supervisor: Aneeqa Noor   Signature:

Date: 21 - Aug - 2024

21 - Aug - 2024

Head of Department   Date

COUNTERSINGED

21 - Aug - 2024

Date   Dean/Principal

CERTIFICATE OF APPROVAL

This is to certify that the research work presented in this thesis, entitled "Investigating the Neuroprotective Effects of Chenodeoxycholic Acid in MPTP-induced Parkinson's disease in BALB/c mic" was conducted by Ms. Mehwish Mehreen under the supervision of Dr. Aneeqa Noor. No part of this thesis has been submitted anywhere else for any other degree. This thesis is submitted to the School of Mechanical and Manufacturing Engineering in partial fulfillment of the requirements for the degree of Master of Scie   in Field of Biomedical Sciences Department of Biomedical engineering and Sciences, National University of Sciences and Technology, Islamabad.

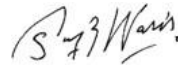Student Name: Mehwish Mehreen   Signature:

Supervisor Name: Dr. Aneeqa Noor   Signature: _____

Name of Dean/HOD: Dr. Muhammad Asim Waris   Signature: _____

AUTHOR'S DECLARATION

I <u>Mehwish Mehreen</u> hereby state that my MS thesis titled "Investigating the Neuroprotective Effects of Chenodeoxycholic Acid in MPTP-induced Parkinson's disease in BALB/c mice" is my own work and has not been submitted previously by me for taking any degree from National University of Sciences and Technology, Islamabad or anywhere else in the country/ world. At any time if my statement is found to be incorrect even after I graduate, the university has the right to withdraw my MS degree.

Name of Student:<u>   Mehwish Mehreen   </u>

Date: <u>   26-08-2024   </u>

PLAGIARISM UNDERTAKING

I solemnly declare that research work presented in the thesis titled "Investigating the Neuroprotective Effects of Chenodeoxycholic Acid in MPTP-induced Parkinson's disease in BALB/c mice" is solely my research work with no significant contribution from any other person. Small contribution/ help wherever taken has been duly acknowledged and that complete thesis has been written by me.

I understand the zero tolerance policy of the HEC and National University of Sciences and Technology (NUST), Islamabad towards plagiarism. Therefore, I as an author of the above titled thesis declare that no portion of my thesis has been plagiarized and any material used as reference is properly referred/cited.

I undertake that if I am found guilty of any formal plagiarism in the above titled thesis even after award of MS degree, the University reserves the rights to withdraw/revoke my MS degree and that HEC and NUST, Islamabad has the right to publish my name on the HEC/University website on which names of students are placed who submitted plagiarized thesis.

Student Signature:

Name: **Mehwish Mehreen**

I dedicate this work to my late mother. With deep love and gratitude, I honor your memory and the many ways you supported and encouraged me. Your constant belief in me has been the foundation of all my achievements. Though you are no longer here, your spirit continues to inspire and guide me every day. This thesis is a testament to your lasting impact on my life. You are deeply missed.

ACKNOWLEDGEMENTS

TABLE OF CONTENTS

LIST OF TABLES

LIST OF FIGURES

LIST OF ABBREVIATIONS, SYMBOLS AND ACRONYMS

PD	Parkinson's Disease
CDCA	Chenodeoxycholic Acid
MPTP	1-methyl-4-phenyl-1,2,3,6-tetrahydropyridine
BDNF	Brain-derived Neurotrophic Nactor
FXR	Farsenoid X-Receptor
CA	Cholic Acid
ALS	Amyotrophic Lateral Sclerosis
MS	Multiple Sclerosis
GUDCA	Glycoursodeoxycholic Acid
TUDCA	Tauroursodeoxycholic Acid
UDCA	Urodeoxycholic Acid
DCA	Deoxycholic Acid
LCA	Lithocholic Acid
AD	Alzheimer's Disease
CTX	Cerebrotendinous Xanthomatosis
6-OHDA	6-Hydroxy Dopamine
GDNF	Glial Cell Line-Derived Neurotrophic Factor
RT-PCR	Real Time Polymerase Chain Reaction

ABSTRACT

Parkinson's disease (PD) remains a major challenge in the field of neurodegenerative diseases and requires innovative therapeutic approaches. In this study, we investigated the therapeutic potential of chenodeoxycholic acid (CDCA) in PD using a 1-methyl-4-phenyl-1,2,3,6-tetrahydropyridine (MPTP)-induced mouse model. CDCA, a naturally occurring bile acid, has previously shown promise in various neurological disorders by reducing neuronal degeneration and promoting neuronal health, however its utility in PD has not been studied. Mice were divided into a control group, an MPTP-induced PD model (20 mg/kg, intraperitoneally) and a treatment group injected intraperitoneally with CDCA (90 mg/kg). CDCA reduced motor impairment and ameliorated anxiety-like behavior as assessed by the pole test and open field test, demonstrated antidepressant effects in the forced swim test and tail suspension test, and results of the Y-maze test showed improved cognitive performance. Furthermore, the effective defense against MPTP-induced dopaminergic degeneration was provided by CDCA through improving the morphological and histological features of neurons in the midbrain, hippocampus, cortex and cerebellum. Additionally, the biomarkers used in this study are brain-derived neurotrophic factor (BDNF) and α-synuclein. Hence, treatment with CDCA significantly mitigated MPTP-induced elevations in α-synuclein levels, indicating that it may have potential to preserve and recover neuronal function. Moreover, the neurotrophic role of CDCA was demonstrated by improving the low levels of BDNF in the presence of MPTP. The results of this study promise valuable insights into the potential therapeutic properties of CDCA in reducing the effects of PD and provide a basis for further research into bile acid-based treatments in neurodegenerative diseases.

Keywords: Chenodeoxycholic acid**,** 1-methyl-4-phenyl-1,2,3,6-tetrahydropyridine, Brain derived neurotrophic factor, α-synuclein, Parkinson's disease**.**

CHAPTER 1: INTRODUCTION

1.1 Bile acids

Bile acids are cholesterol-derived acidic steroids, manufactured within the liver and then housed in the gall bladder and released into the Gastrointestinal Tract to aid in postprandial nutrient absorption. Through enterohepatic circulation, they are reabsorbed from the intestines back to the liver, playing a crucial role in maintaining homeostasis. Additionally, Bile acids, acting as steroid hormones, impact glucose, lipid, and energy metabolism through the activation of nuclear receptors like the Takeda G Protein Coupled Bile Acid Receptor 5 and Farsenoid X Receptor (FXR) [1]. In peripheral tissues such as the liver, skeletal muscle, pancreas, and brown and white adipose tissue, these receptors are activated by bile acids to regulate glucose and lipid metabolism. Recent research indicates that the central nervous system contains 20 different types of BAs. Specifically, the brain's essential requirement includes the presence of two primary bile acids, CDCA and cholic acid (CA) [2]. In the adult liver, cholesterol is converted to bile acids every day by about 500 mg. The classic or neutral bile acid pathway, which occurs in the liver, and the alternate or acidic bile acid pathway, which occurs in peripheral tissues and in the liver, are two major bile acid synthetic pathways [3]. This classic pathway is the main route for bile acid production, mainly involving the enzyme cholesterol 7α-hydroxylase (CYP7A1) and accounts for approximately 90% in humans and around 75% in mice. This pathway initiates cholesterol conversion into 7α-hydroxycholesterol by the enzyme CYP7A1, a microsomal cytochrome P450 enzyme found exclusively in the liver [4].

1.2 Bile acids in neurodegenerative diseases

Neurodegenerative diseases, impacting millions globally, result from a range of factors. Although the specific causes differ, a common issue is the buildup of misfolded or mutated proteins. These factors lead to greater dysfunction, significant loss of neurons, and brain shrinkage [5]. Bile acids have been implicated in the advancement or initial phases of Alzheimer's disease (AD). A recent study has pinpointed glycoursodeoxycholic acid (GUDCA) as a blood-based biomarker capable of accurately predicting the onset of AD and mild cognitive impairment. GUDCA exhibits notable neuroprotective effects by effectively suppressing glutamate release and reducing glutamate excitotoxicity in neuronal cells [6]. In both experimental animal models and clinical studies of PD and AD, tauroursodeoxycholic acid (TUDCA) and ursodeoxycholic acid (UDCA) have shown

promise in protecting nerve cells. These acids have been shown to protect neurons from degeneration and enhance cognitive function in PD and AD. Their neuroprotective effects are thought to occur through mechanisms such as reducing oxidative stress, preventing apoptosis, and regulating inflammation [5].
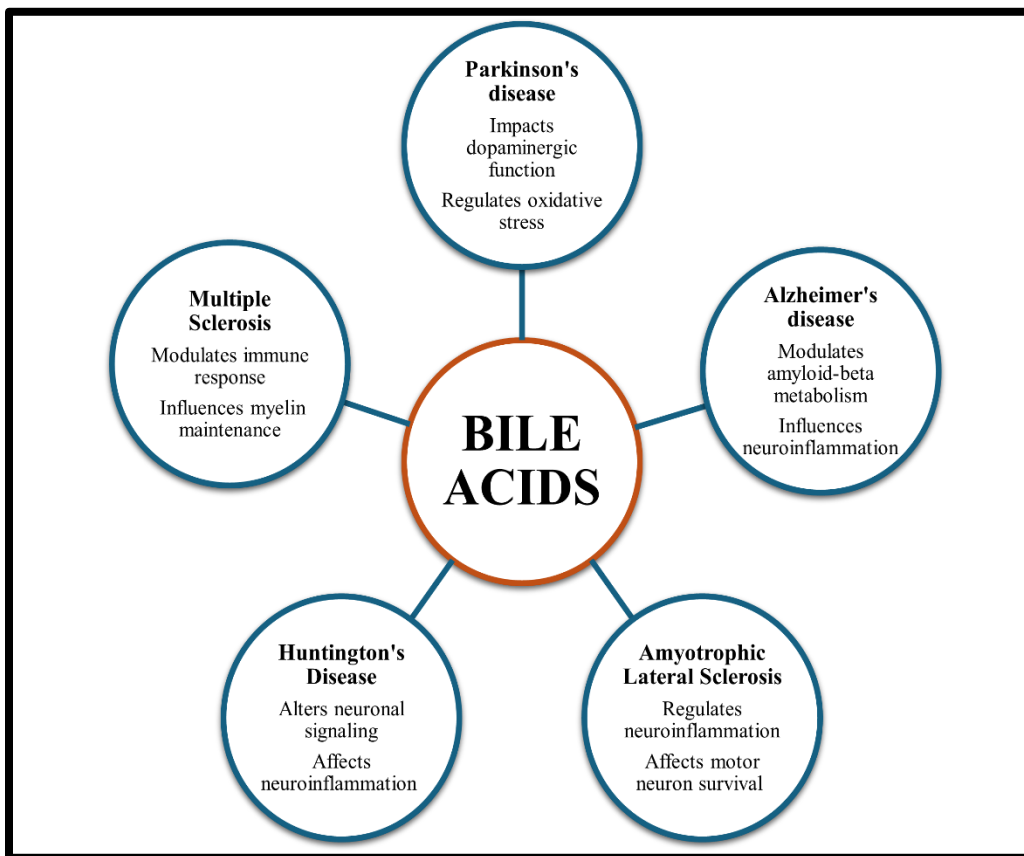
Figure 1.1. Role of bile acids in neurodegenerative diseases. The diagram demonstrates the role of bile acids in five primary neurodegenerative conditions: AD, PD, Huntington's disease, Amyotrophic Lateral Sclerosis (ALS), and Multiple Sclerosis (MS). It emphasizes the biochemical mechanisms by which bile acids impact the advancement of these diseases, including their influence on neuroinflammation, oxidative stress, mitochondrial dysfunction, and the survival of neurons.

Tauroursodeoxycholic acid (TUDCA) extends its effects beyond PD and AD to also influence ALS. It achieves this by reducing oxidative stress, inhibiting the apoptotic cascade, protecting mitochondria, and exerting an anti-neuroinflammatory action. A study that administered varying doses of ursodeoxycholic acid (UDCA, a form of TUDCA) to ALS patients yielded notable findings on the drug's pharmacokinetic profile and its ability to penetrate the central

nervous system. The study demonstrated the dose-dependent crossing of UDCA through the blood-brain barrier [7]. TUDCA and ursodeoxycholic acid UDCA exhibit therapeutic promise in prion disease by reducing PrP conversion, neuronal loss, and astrocytosis. They accomplish this by diminishing PrP conversion in cell-free assays and infected cell cultures, as well as reducing the seeding ability of PrP Sc. Both TUDCA and UDCA also effectively reduce neuronal loss in prion-infected cerebellar slices and astrocytosis in prion-infected mice, particularly in males, suggesting gender-specific differences in drug metabolism. These compounds are FDA-approved for human use, making them promising treatments for prion diseases [8].

The impact of microbiota-modified bile acids on neurodegenerative diseases has been evaluated previously. Deoxycholic acid (DCA) and lithocholic acid (LCA), derived from CA and CDCA, have been found to influence intracellular organelles and play a role in these diseases. Specifically, DCA and LCA activate mitofusin 2 facilitating mitochondria and endoplasmic reticulum fusion, thereby enhancing ATP synthesis. At normal concentrations, these bile acids promote mitochondrial fusion, a critical process for ATP generation. Additionally, DCA and UDCA stimulate autophagy, whereas primary bile acids such as CA, CDCA, and taurocholic acid inhibit this process [9]. In ALS patients TUDCA demonstrated good tolerability without significant adverse effects. TUDCA exhibits cytoprotective and anti-apoptotic properties suggesting potential neuroprotective effects. Its neuroprotective mechanisms likely involve inhibiting mitochondrial-associated apoptosis and modulating specific targets related to apoptosis. TUDCA's role in ALS may revolve around its ability to shield cells from apoptosis and regulate mitochondrial function, contributing to its neuroprotective capabilities [10].

1.3 CDCA and neurodegenerative diseases

CDCA, a primary bile acid synthesized in the liver, originates from a precursor, cholesterol. The conversion of cholesterol to primary bile acids depends on a specific group of cytochrome P450 enzymes found in various cellular compartments. The classical pathway for bile acid synthesis begins with 7α-hydroxylase (CYP7A1), which transforms cholesterol into 7α-hydroxycholesterol. Then, sterol 27-hydroxylase (CYP27A1) is responsible for converting these intermediates into primary bile acids like CDCA [11].
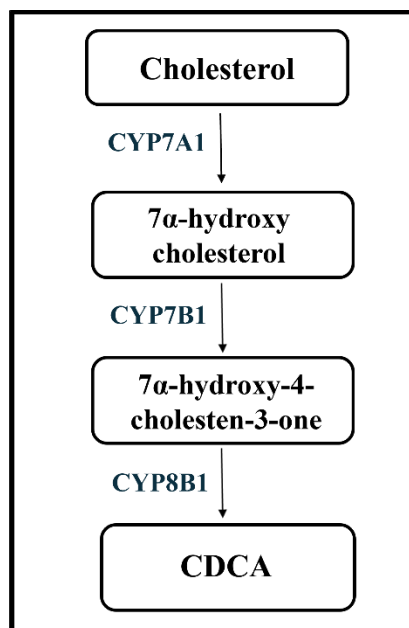
Figure 1.2. Classical pathway of synthesis of CDCA. The diagram illustrates the transformation of cholesterol into CDCA via a series of three enzymatic steps, which includes the involvement of CYP7A1 (cholesterol 7α-hydroxylase), CYP7B1 (oxysterol 7α-hydroxylase), and CYP8B1 (sterol 12α-hydroxylase).

CDCA has gained significant attention for its potential therapeutic effects in neurodegenerative diseases. CDCA exhibits multifaceted pharmacological properties, including anti-inflammatory, antioxidant, and neuroprotective actions [12]. It exhibits neuroprotective effects attributed to its ability to enhance insulin signaling, regulate amyloid-beta metabolism, and promote neurotrophic signaling pathways. By improving insulin sensitivity in the hippocampi of AD rats through mechanisms such as reducing pSer307-IRS1 phosphorylation and increasing Akt activation, CDCA shows promise as a therapeutic agent for AD management [13]. It is also used for treating cerebrotendinous xanthomatosis (CTX), an uncommon condition characterized by lipid accumulation due to mutations in the CYP27A1 gene. a rare lipid storage disorder caused by mutations in the CYP27A1 gene. These mutations disrupt synthesis of bile acids, leading to decreased production of CDCA [14].

Moreover, CDCA has been found to effectively prevent axonal degeneration in CTX and Early initiation of CDCA treatment has shown significant benefits in improving the morbidity and prognosis of CTX patients [15]. As a result, CDCA replacement therapy has been approved to

treat CTX. However, the effectiveness of CDCA treatment diminishes once severe neuropsychiatric symptoms develop. Therefore, early diagnosis and starting CDCA therapy as soon as possible are vital for improving outcomes in patients with CTX [14]. The exploration of bile acid in the context of cognitive impairment in PD is an understudied area, and uncertainties persist regarding its specificity and sensitivity as a biomarker for early diagnosis. Addressing this gap, the researchers conducted a metabolomics analysis of plasma bile acids in patients with PD-MCI (PD with Mild Cognitive Impairment) and PD-NC (PD with Normal Cognition). The results of the study revealed significant decreases in CA, CDCA, and UDCA in patients with PD-MCI compared to those with normal cognition [16]. This groundbreaking research sheds light on potential alterations in the bile acid profile associated with cognitive changes in PD, emphasizing the need for further exploration in this realm for potential diagnostic implications.

1.4 Parkinson's disease

PD is a long-term, progressive neurodegenerative condition. The signs and symptoms are believed to become prominent when the nerve cells belonging to an area of the brain become impaired or die. The brain region called the basal ganglia, produces the chemical dopamine. When dopamine production is compromised, the patients experience movement problems which can take the form of tremors, muscle stiffness, slowness of movements, and impaired balance and coordination [17]. In addition to these, the non-motor symptoms, such as problems with memory, feelings of sadness, seeing things that aren't real, difficulties with body functions like heart rate, and trouble sleeping, there exists a significant burden of symptomatic complications [18].

The main clinical symptoms of PD arise from the loss of dopaminergic neurons in the substantia nigra of the midbrain [19]. Dopamine neurons are particularly vulnerable to oxidative stress, which is caused by increased reactive oxygen species and a weakened antioxidant defense system [20]. This link between oxidative stress and PD is further supported by animal models using neurotoxins such as MPTP, rotenone, and 6-hydroxydopamine (6-OHDA). These models generate reactive oxygen species, which contributes to the gradual loss of dopaminergic neurons [21].

1.4.1 Etiology and pathogenesis of PD

The exact cause of PD is not completely clear. However, autopsies often reveal Lewy bodies, which are aggregates of α-synuclein proteins, play a role in the damage to neurons in the substantia

nigra. Because of this, PD is classified under neurodegenerative diseases known as synucleinopathies [22]. The cause is not entirely known, but both genetic and environmental factors are important. Gene mutations in proteins related to protein handling, oxidative stress, and mitochondrial function have been identified in familial PD. Environmental toxins used in PD animal models also affect mitochondrial function and increase free radicals, contributing to protein aggregation [23].

While numerous factors associated with PD causation have raised interest in its environmental component, the discovery of the neurotoxic effects of MPTP was a pivotal moment in PD research. This finding not only spurred studies to unravel its mechanism of action and its relevance to PD pathogenesis but also provided a valuable model for studying motor deficits in primates and testing drug efficacy in humans. It's important to note, however, that MPTP-induced parkinsonism, while a useful model, differs from PD in humans because it is not progressive and does not lead to Lewy body formation [24]. Hence, PD remains a complex interplay of genetic and environmental factors, with ongoing research into its mechanisms and potential treatments.

1.4.2 Epidemiology of PD

PD is a condition associated with age that is becoming more prevalent globally as populations age. Its recognition as a distinct clinical entity date back to the 19th century, with its pathology elucidated in the first half of the 20th century. PD became a significant medical challenge during and following the mid-20th century [25]. PD demonstrates a higher prevalence in males worldwide, with its occurrence increasing with age. This pattern is more pronounced in western countries than in Asian nations. These variations in prevalence are influenced by a combination of genetic and environmental factors. Within a single country, different ethnic populations may exhibit varying rates of PD incidence, indicating a genetic component to the disease's risk. Moreover, the elevated incidence of PD among Japanese and African populations in the Americas compared to their home countries suggests an environmental impact on PD development [26].

In terms of cognitive functions in PD, cognitive changes are increasingly recognized even appearing in its early stages. PD-MCI affects 20% to 40% of patients, while the incidence of PD-related dementia rises with disease duration, reaching over 80% after 20 years. Factors linked to cognitive decline in PD include older age, the progression of the disease, difficulties with walking,

autonomic dysfunction, and experiencing hallucinations, REM behavior disorder, and neuropsychological test results indicating posterior predominant dysfunction [27].

1.4.3 Clinical characteristics of PD

PD often manifests with a loss of dexterity or, less frequently, a subtle dragging of one foot. Its onset is typically gradual, and the initial symptoms may go unnoticed or be misinterpreted for an extended period [28]. Initial symptoms of PD encompass a range of manifestations, with constipation being the most prevalent. Other indicative signs include experiencing vivid dreams and acting them out during the rapid eye movement phase of sleep, which may suggest the presence of REM sleep behavior disorder. Additionally, individuals may notice a decreased sense of smell (hyposmia), asymmetric vague shoulder pain, or symptoms of depression [29].

The primary characteristics of PD are bradykinesia, rigidity, rest tremor and gait impairment, while bradykinesia is often the most debilitating symptom in the early stages [30]. The motor features in PD can vary widely, leading to efforts to categorize subtypes. Two main subtypes are commonly observed: tremor-dominant Parkinson's and non-tremor-dominant Parkinson's. These subtypes may have different causes and development pathways, though a clear classification consensus is still lacking [31].

1.4.4 Modelling PD in animals

Over the last few decades, researchers have utilized various types of animal models to study PD. These models generally fall into two categories: those induced by environmental or synthetic neurotoxins and those created by introducing PD-related genetic mutations in vivo [32]. Current animal models of PD are not able to completely replicate PD and its full range of pathology and symptoms. The main reason for this limitation is that each model is designed to induce only a limited set of pathological processes seen in PD. These processes are often either artificially induced in a manner that does not fully reflect the disease, as in toxin models, or they may be relevant to PD but represent only a fraction of the overall pathology [33].

Many of the PD models involve inducing degeneration of dopaminergic neurons using neurotoxins. The first neurotoxin used was 6-OHDA, initially intended for degenerating sympathetic nerves and later adapted for modeling PD in the brain. Another neurotoxin, MPTP, was discovered when cases of chemically induced parkinsonism emerged after a failed attempt to

synthesize the opioid drug MPPP [34]. The discovery of MPTP, a synthetic compound with heroin-like properties that is toxic to dopamine neurons, made it one of the most commonly used toxins in modeling the characteristics of PD [35]. The timing of MPTP administration in mice greatly affects the results. MPTP is usually given through repeated intraperitoneal or subcutaneous injections, as intravenous injections are no longer used. If injections are given closely together within a single day, the impact on dopamine-producing neurons can increase [36]. Studies show that giving multiple injections in a single day is known as an acute administration regimen. In contrast, administering one injection per day over several days or weeks is referred to as a subacute or chronic administration regimen. The comparison between both regimens shown in table 1.1 [37].

Table 1.1. The comparison between the two most common and widely used regimens of MPTP.

MPTP model type	Injection route	Duration of protocol	Loss of dopaminergic neurons
Acute (14-20mg/kg)	Intraperitoneal	Four doses in a single day with interval of two hours	40-90% striatal dopamine depletion
Subacute (30mg/kg)	Intraperitoneal	Single dose for five consecutive days	40-50% striatal dopamine depletion

1.4.5 Diagnosis of PD

The current diagnosis of PD relies on clinical features gathered from medical history and examination, as well as the patient's response to dopamine medications and the emergence of motor fluctuations over time [38]. PD should be considered if an individual display one or more of its cardinal features, which include bradykinesia, resting tremor, rigidity, and in later stages, postural instability. The presence of a characteristic resting tremor significantly raises the suspicion for PD, although around 20% of patients do not develop this tremor [39].

A concise set of research criteria for diagnosis of PD includes [40].

1. Evidence of disease progression.
2. Two of the three cardinal features (tremor, rigidity, bradykinesia).
3. Two of the following:

a. Significant response to L-dopa

   b. Signs of asymmetry

   c. Asymmetrical onset

4. No clinical signs pointing to an alternative diagnosis.

5. No known cause for similar features

Additionally, diagnostic tools like brain imaging (e.g., MRI, CT) and dopamine transporter imaging (e.g., DaTscan) can aid in confirming the clinical diagnosis of PD and ruling out conditions with similar symptoms. Genetic testing may also be considered in select cases, as advancements in PD genetics have identified specific mutations associated with the disease. A comprehensive assessment that includes clinical evaluation, imaging modalities, and genetic testing contributes to a more precise diagnosis of PD [41].

1.4.6 Treatment of PD

There is currently no cure for PD, as existing therapies are unable to stop or reverse its progression. However, various medications are available to manage its symptoms. These drugs work by either increasing dopamine levels in the brain or replicating the effects of dopamine [42]. As we know the key pathological feature of PD is the accumulation of abnormal α-synuclein aggregates. One potential approach to halt the spread of α-synuclein is the use of antibodies that target and degrade extracellular α-synuclein, preventing its transmission to nearby cells. An example is prasinezumab (PRX002, Prothena), a humanized monoclonal antibody which has demonstrated a reduction of approximately 97% in free serum α-synuclein levels and has shown good tolerance in phase I clinical trials [43].

Current approved treatments for PD focus on elevating dopamine levels in the striatum to alleviate motor symptoms [44]. The primary strategy in treating PD is to address the dopamine deficiency by supplying levodopa, the natural precursor of dopamine. Additionally, other oral medications can be utilized either alone or in combination [45]. Another promising frontier in PD research is gene therapy which has potential for both neuroprotection and neurorestoration in PD. Innovative approaches include gene therapy targeting subthalamic glutamic acid decarboxylase and the application of glial cell line-derived neurotrophic factor (GDNF) [46]. Direct delivery of GDNF has demonstrated symptom reduction in PD patients, facilitated by a tetracycline-controlled transactivator. Other gene therapy strategies, not aimed at altering disease progression, involve a

tricistronic system incorporating aromatic L-amino acid decarboxylase, tyrosine hydroxylase, and GTP cyclohydrolase 1 to collectively enhance dopaminergic enzyme expression [47]. Numerous medications are currently in various stages of clinical trials, and with the continued advancement of new therapies, significant progress in the treatment of PD is expected to progress significantly in the near future [48].

1.4.7 Bile acids in treatment of PD

In the context of managing neurodegenerative disorders like AD and PD, bile acids have been explored as potential remedies. As discussed in a patent, promisingly, 2-fluorinated bile acid compounds show potential by reducing inflammation, boosting mitochondrial function, and aiding in the clearance of toxic proteins associated with these diseases. This avenue holds significant promise as a therapeutic approach for neurodegenerative disorders [49]. UDCA and TUDCA are hydrophilic bile acids that demonstrate potential as antiapoptotic agents, making them subjects of research for treating neurodegenerative disorders like PD. Presently, two small clinical trials are underway to evaluate the potential of UDCA in slowing the progression of PD [50].

In the extensive examination conducted by Ackerman and Gerhard, the authors systematically reviewed outcomes from diverse studies involving cell lines, animal models, and human subjects. These results emphasize the significant potential of bile acids in addressing various neurodegenerative disorders. Interestingly, among the investigated bile acids, CDCA has not yet been explored as a potential candidate for PD [6]. This notable gap in the current research landscape highlights the need for further investigations into the specific role of CDCA in the context of PD treatment.

1.5 Aims and Objectives

The precise mechanisms underlying CDCA's neuroprotective effects in PD, as well as its long-term safety and efficacy in clinical settings, have yet to be fully investigated. With its neuroprotective properties, CDCA is a good option for treatment of PD especially in MPTP-induced mouse models. Research aims to determine whether CDCA can successfully improve cognition, increase synaptic plasticity and neurogenesis, decrease neurodegeneration, and can improve neurotrophic factors related to PD. Preclinical research on the application of CDCA in the treatment of PD may result in clinical trials that allow for the investigation of the best possible

dosage, timing, and combination strategies, thereby improving the management and rehabilitation of PD. The research's goals and objectives are as follows:

1. Development of PD model using MPTP and to investigate the therapeutic potential of CDCA in PD models.
2. Evaluation of effects of CDCA by conducting behavioral tests.
3. Assessment of histological and morphological changes in the brain regions of mice through H&E staining.
4. Determining whether CDCA affects the biochemical markers linked to PD and has neuroprotective benefits.

CHAPTER 2: MATERIALS AND METHODOLOGY

2.1 Experimental timeline and overview

In this study, we employed a comprehensive experimental approach to study the effects of CDCA on PD in animal models. The experimental schedule shown in Figure 2.1 outlines the sequential steps of this study. First, the animals were divided into groups. Once grouping was completed, we started to develop an animal model mimicking PD. After the model was created, the animals received the intended treatment according to the experimental protocol. After the treatment phase, we performed behavioral tests to evaluate the functional outcome and potential treatment effects. Finally, animals were humanely sacrificed and dissected so that tissue samples could be collected for further analysis using polymerase chain reaction (PCR) and histopathology.
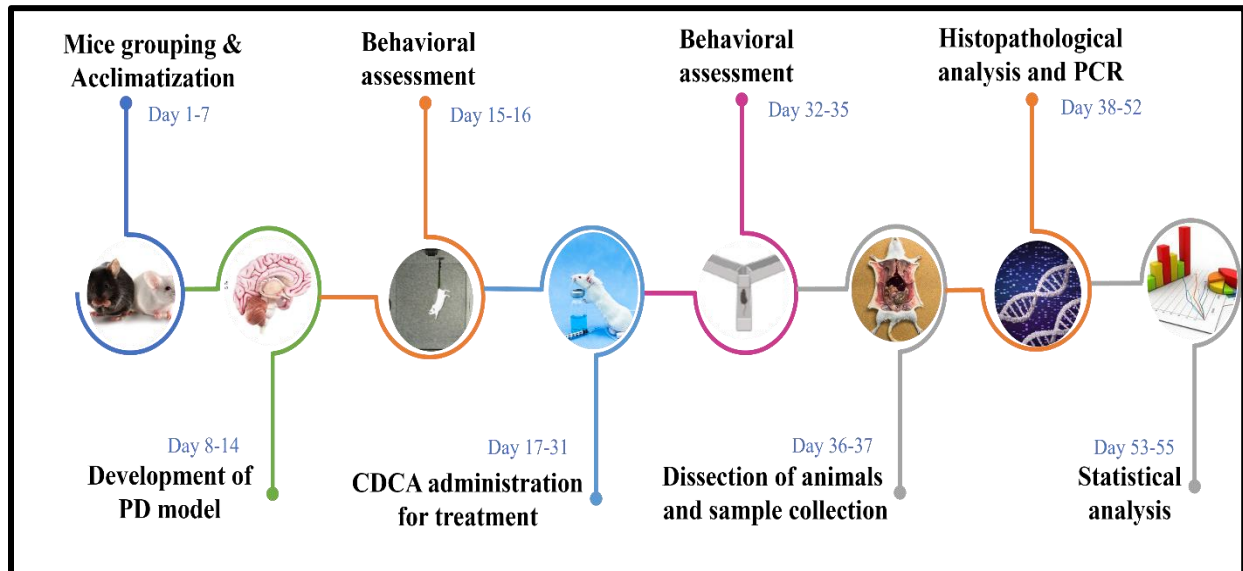
Figure 2.1. Experimental design. The figure illustrates the experimental process starting with the acclimatization of mice, induction of disease, administration of treatment, behavioral analysis, sacrifice of animals, histopathological examination, PCR analysis, and statistical evaluation. Each stage is portrayed in sequence to demonstrate the thorough methodology used in the research.

2.2 Ethics statement

All experimental procedures followed the National Institutes of Health guidelines for the care and use of animals and were approved by the NUST Institutional Review Board (IRB No. 2024-IRB-

A-01/01). Male BALB/c adult mice (7-8 weeks old) were purchased from the National Institute of Health Sciences, Islamabad, Pakistan.

2.3 Drugs and materials

All the chemicals and material used in the study are listed here, along with their sources, to ensure transparency and provide important reference information for repeatability.

Table 2.1. List of drugs, chemicals and other material along with their sources.

	Name	Source	Identifier
1.	CDCA	Macklin, China	CAS: 474-25-9
2.	MPTP	Macklin, China	CAS: 23007-85-4
3.	Sodium Bicarbonate	Sigma Aldrich, USA	CAS: 144-55-8
4.	TRIzol isolation reagent	Fine Biotech Life Sciences, UK	Cat. No. FTR-100
5.	Reverse Transcriptase	Thermo Fisher Scientific, Lithuania	Cat. No. EP0441
6.	2% Agarose Gel	Sigma Aldrich, USA	CAS: 39346-81-1
7.	10X TBE buffer	Solarbio, China	Cat. No. T1050
8.	PCR master mix	Wizbio Solutions, South Korea	Cat. No. W1401-2
9.	SYBR green master mix	Wizbio Solutions, South Korea	Cat. No. W1711

2.4 *In silico* analysis

In silico analysis was performed before starting the experimental work in the lab and animal house. The 3D structures of α-synuclein (UniProt ID: 10133) and BDNF (UniProt ID: P21237) were obtained from AlphaFold, while the chemical structure of CDCA (PubChem CID: 10133) was retrieved from the PubChem database. These structures were cleaned using Discovery Studio Visualizer 3.0. Docking was conducted using PyRx 0.8 to understand the structural interactions between BDNF, α-synuclein, and CDCA, and to calculate their binding affinities. The interactions between BDNF-CDCA and α-synuclein-CDCA were visualized using Discovery Studio Visualizer 3.0, highlighting key interaction patterns.

2.5 Animal grouping and treatment

The mice were housed at the NUST Animal House under standardized condition, 12 hours of dark and 12 hours of light. They were kept in cages equipped with a water bottle and a petri dish for food. The mice were randomly divided into three groups, with six mice in each group.

 i.   Healthy group: Mice received the drug vehicle.
 ii. Diseased group: Mice treated with MPTP to induce a PD animal model.
 iii. Treatment group: Mice treated with MPTP followed by administration of CDCA.

2.6 Dosing protocol of MPTP

The mice were acclimated for a week before starting MPTP induction. They were weighed and sorted a day before the induction began. We followed the standard regimen, administering one injection of MPTP every 2 hours, totaling four doses over an 8-hour period in one day. An acute dose of 20 mg/kg MPTP was injected intraperitoneally into eight-week-old male mice. Behavioral tests were conducted on day 15 and 16.

2.7 Dosing protocol of CDCA

A dose of 90 mg/kg/day of CDCA was used. A CDCA suspension was prepared with 8.4% (1 mmol/mL) NaHCO3 [13]. The injection volumes were adjusted according to the body weight of the mice. After MPTP induction, behavioral tests were conducted and then the administration of CDCA began, with intraperitoneal injections given daily for 14 days. Behavioral tests were conducted on the day after the final dose of CDCA.

Figure 2.2. Intraperitoneal injection Procedure in Mice. The figure illustrates a method to administer intraperitoneal injection in a mouse. It depicts the position of the needle and the injection site in the abdominal cavity.

2.8 Behavioral analysis

Behavioral tests were conducted after both MPTP and CDCA administration. Following MPTP induction, initial behavioral assessments were performed to evaluate the baseline effects of MPTP on the mice. These tests included the tail suspension test and open field test to monitor any MPTP-induced motor and behavioral impairments. After completing the initial assessments, CDCA treatment began and continued daily for 14 days. Upon completing the CDCA treatment regimen, another set of behavioral tests was conducted to evaluate any improvements or changes in motor function and overall behavior due to CDCA. The same tests (tail suspension and open field) were repeated to maintain consistency and comparability between the pre- and post-CDCA administration phases. Additionally, three more tests were added after CDCA treatment: the forced swim test, the pole test and the Y-maze test.

2.8.1 Tail suspension test

The tail-suspension test is a behavioral experiment conducted on mice. It helps screen potential antidepressant drugs and assesses other interventions that may influence behaviors associated with depression [51]. For this test, each mouse from each group was individually suspended by its tail from a horizontal bar using adhesive tape for a secure hold. The test was conducted for a duration of 6 minutes per mouse. During this time, we observed and recorded the duration of immobility (Immobility time is defined as the period when the animal hangs quietly and without movement) [52] using a stopwatch and a video camera.

Figure 2.3. Tail Suspension Test setup with Mouse. The figure shows the tail suspension test where a mouse is hung by tail to a horizontal stand bar using adhesive tape, to access depressive-like behavior.

2.8.2 Open field test

Open field test is widely recognized as one of the most frequently used behavioral tests in animal psychology. It is used to evaluate general locomotor activity and anxiety-related behavior in mice. [53]. The apparatus was built with a 60×60 cm white wooden cage, 60 cm tall walls and 16 equal-sized squares of 15×15 cm each. Each mouse was placed in the center of an open field apparatus. Upon release, the timer was started, and the mouse was allowed to explore for five minutes. The session was recorded on video and later analyzed manually. We documented the total the time spent in the center versus the periphery, and the number of entries into central and peripheral areas. After each mouse, the apparatus was cleaned with 70% ethanol.

Figure 2.4. Open Field Test setup with Mouse. The figure shows a mouse in an open field apparatus to access locomotion and anxiety-like behavior.

2.8.3 Pole test

Pole test is an indicator of bradykinesia [54]. So, to assess motor coordination and balance in mice, we conducted this test. The mice underwent a training period of three days before the

commencement of the formal experiment. We placed each mouse at the top of the pole facing upwards and started the timer as soon as the mouse was released. We measured the time it took for the mouse to turn 180° on the pole. The session was videotaped, and it was then manually analyzed.

Figure 2.5. Mouse on pole for pole test. The figure shows a mouse positioned on a vertical pole in upward direction to evaluate turn time.

2.8.4 Forced swim test

The forced swim test, also known as the 'behavioral despair' test, serves as a rodent model to predict the effectiveness of antidepressant drugs [55]. Both the forced swim test and the tail suspension test are used as models for rodent depression. These tests primarily measure a decrease in locomotor activity along with other mobility-related behaviors [56]. Transparent cylinders, about 25-30 cm tall to keep mice from touching the bottom, were used in this study. The water temperature was kept steady at around $25 \pm 1°C$. Each mouse was gently placed by its tail into the water-filled cylinder for a 6-minute test where escape wasn't possible. The first 2 minutes weren't counted because most mice swam continuously. We only looked at the last 4 minutes to see how long the mice stayed still or floated, not counting any time they spent swimming or trying to climb

out. Afterward, the mice were dried off with a towel and returned to their cage for a 10-minute observation period.

Figure 2.6. Mouse in cylinder for Forced Swim Test. The figure shows a mouse placed in a water-filled cylinder to access depressive-like behavior and immobility in forced swim test.

2.8.5 Y maze test

The Y-maze test evaluates spatial memory by having mice explore a maze with three arms shaped like a "Y" [57]. In this test, a Y-shaped apparatus was used constructed of a wooden box wrapped in a black sheet. The apparatus is comprised of two arms labeled as familiar and one arm labeled as novel. The three arms that make up this apparatus measure 30 cm in length, 8 cm in width, and 15 cm in height and they are inclined at a 120-degree angle. During the training phase, which lasted 10 minutes, mice were placed in the familiar arms, and the novel arm was blocked. After a one-hour break, the testing phase began, lasting 5 minutes, during which the novel arm was accessible [58]. We analyzed video recordings to analyze the percentage of alternations. The formula used to calculate the percentage of spontaneous alternation was [(number of alternations)/(total number of arm entries − 2)] × 100 [59]. This procedure was carried out across all mice of all groups.

Figure 2.7. Mouse in Y maze apparatus for memory testing. The figure shows a mouse in a Y-maze device, which is used to measure cognitive ability and spatial memory by observing how the mouse moves around the maze.

2.9 Histopathological analysis

Histopathological analysis was carried out to observe the morphological changes and histological patterns in the cellular structures of the brain, which involves studying tissues at a microscopic level.

2.9.1 Tissue preparation

The day after conducting behavioral experiments, tissue dissection and fixation were performed. For histological analysis, mice were anesthetized intraperitoneally with ketamine at a dose of 100 mg/kg [60]. Following anesthesia, an incision was made in the abdominal cavity to expose the heart. A needle was inserted into the right ventricle while simultaneously making an incision in the right atrium. This allowed for the infusion of 80 ml of 0.9% saline, followed by 100 ml of a fixative solution containing 4% paraformaldehyde in 0.1 M phosphate-buffered saline at pH 7.4 [61]. After perfusion, the brain was carefully removed and rinsed with PBS to eliminate excess fixative and blood. Subsequently, the brain tissue was immersed in a 4% paraformaldehyde fixative solution.
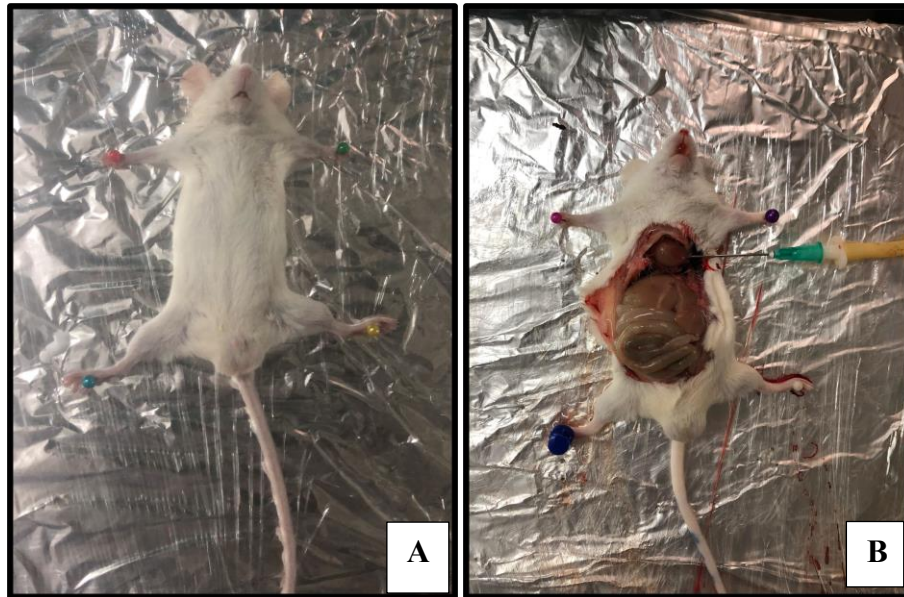
Figure 2.8. Mouse positioning and needle insertion for transcardiac perfusion. Figure A shows how the pinned mouse on a dissecting stage. Figure B shows the insertion of needle in the heart for transcardiac perfusion.

2.9.2 Hematoxylin & Eosin staining and Slides preparation

We further processed the tissue fixed earlier with 4% paraformaldehyde to prepare slides. The first step was dehydration, which involved immersing the tissue in increasing concentrations of ethanol (70%, 95%, 100%) to remove water. After dehydration, we used xylene (CAS No: 1330-20-70, Sigma Aldrich USA), a clearing agent, to remove the alcohol and make the tissue transparent. Next, we cut thin slices of the tissue (3-5µm) using a microtome and rehydrated them by immersing them in decreasing concentrations of ethanol (100%, 95%, 70%). We then stained the rehydrated tissue slices by immersing them in hematoxylin solution for a few minutes.

After staining, we rinsed the slides to remove the excess stain. Bluing was performed by placing the slides in a weak alkaline solution, i.e ammonium water, to stabilize the hematoxylin stain, followed by another rinse. The slides were then immersed in eosin solution for a few minutes to counterstain the tissue and rinsed again. Bluing was performed by simple tap water to stabilize the hematoxylin stain, followed by another rinse. The slides were then immersed in eosin solution for a few minutes to counterstain the tissue and rinsed again. After staining, we dehydrated the tissue again using increasing concentrations of ethanol (70%, 95%, 100%) and cleared it with xylene.

Finally, we applied a mounting medium and placed a cover slip over the tissue sections to preserve them and facilitate microscopic examination.

2.9.3 Microscopic tissue analysis

The slides were observed under a light microscope (Optika B-150, Italy) at magnifications of 10X and 40X to evaluate tissue structure, cell numbers, and cellular patterns. Photomicrographs were taken of the cerebellum, hippocampus, cortex, and midbrain to compare the changes among the three groups. The purpose of the microscopy was to examine the alterations in cell chemistry caused by MPTP induction.

2.10 Gene expression analysis

2.10.1 Fresh tissue dissection

First, mice were anesthetized with injections of ketamine to collect tissue samples for PCR. Once fully anesthetized, the mice were carefully dissected. A cut was made along the skull's length, and the skin was peeled back to each side. The top of the skull was then removed to expose the brain. Using a spatula, the brain was gently lifted out of the skull.
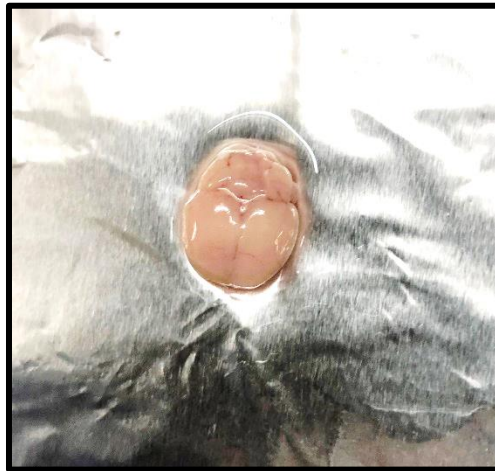
Figure 2.9. Mouse brain post-dissection. The figure shows the brain which was removed from the skull of mouse after dissection.

2.10.2 RNA extraction

Total RNA was extracted from the tissues using the TRIzol isolation reagent. In the first step, 1000 µl of TRIzol was added to sample (80mg), followed by sonication to homogenize it. The mixture

was left at room temperature for 5 minutes. Next, it was centrifuged at 12,000 rpm for 10 minutes at 4°C. The supernatant was then transferred to a new tube, and 200 µl of chloroform was added. After shaking for 30 seconds, the mixture was centrifuged again at 12,000 rpm for 10 minutes at 4°C. The aqueous phase was transferred to a new tube, and 500 µl of isopropanol was added. This was incubated at room temperature for 10 minutes. Following another centrifugation at the same speed and temperature, the supernatant was removed. The remaining pellet was washed with 75% ethanol, vortexed, and centrifuged for 2 minutes. After discarding the wash buffer, the pellet was air-dried for 10 minutes. Finally, the pellet was resuspended in 50 µl of RNase-free water and stored at -80°C until further use.

2.10.3 Evaluating RNA Concentration and Quality

The concentration and quality of the extracted RNA were assessed using a Colibri NanoDrop (TitertekBerthold, Germany). Both the concentration and purity were within acceptable ranges. The absorbance at 260 nm indicated that the RNA concentration was appropriate for our samples. Additionally, the 260/280 nm ratio, which checks for protein contamination, was between 1.8 and 2.0, and the 260/230 nm ratio, which indicates the presence of other contaminants, was between 2.0 and 2.2.

2.10.4 cDNA synthesis

For cDNA synthesis, 2 µl of RNA sample was taken and 6 µl of DNTPs and 1.5 µl of oligo(dT)s was added into it, incubating the mixture at 55°C for 5 minutes. After this, 4 µl of RT buffer, 2 µl of DTT, 1 µl of reverse transcriptase, and 3.5 µl of nuclease-free water were added. The reaction mix was then incubated in a thermal cycler at 42°C for 60 minutes. Once completed, the cDNA was formed and stored at 4°C for later use in gradient and RT-PCR.

2.11 Polymerase Chain Reaction (PCR)

First, the primers were designed for performing gradient and RT-PCR.

2.11.1 Primer designing

The primers chosen, brain BDNF and α-synuclein, were based on information from published sources and they were ordered from Bionics, Islamabad, Pakistan. Next, we used Primer BLAST on the NCBI website to verify if these primers accurately and specifically matched the targets

indicated in figures 2.10, 2.11, 2.12and 2.13. This step ensured that the primers were suitable for use in the PCR.
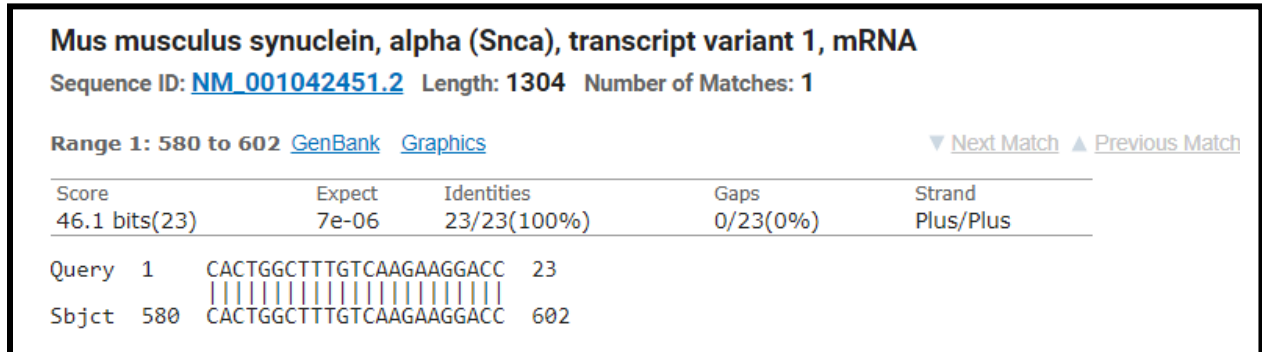
Figure 2.10. BLAST analysis of forward primer of α-synuclein. The figure shows the result of nucleotide blast of forward primer of α-synuclein to check its specificity in *Mus Musculus*.
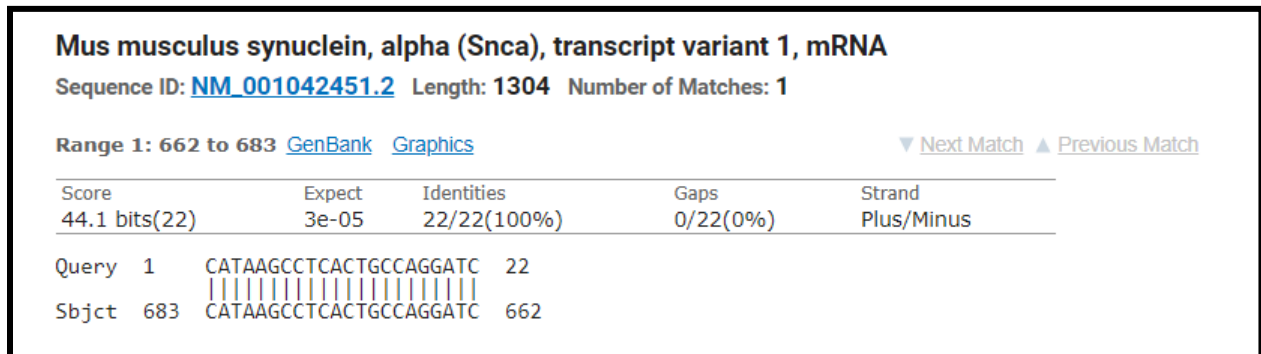
Figure 2.11. BLAST analysis of reverse primer of α-synuclein. The figure shows the result of nucleotide blast of reverse primer of α-synuclein to check its specificity in *Mus Musculus.*
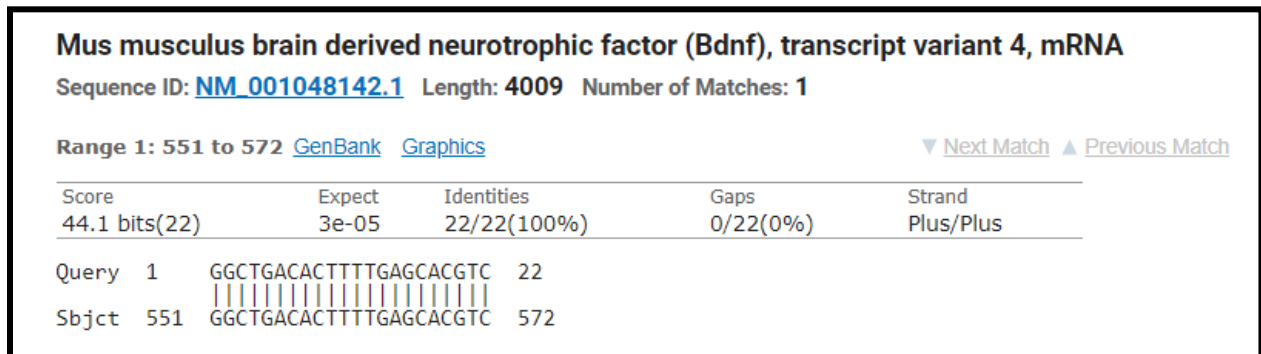
Figure 2.12. BLAST analysis of forward primer of BDNF. The figure shows the result of nucleotide blast of forward primer of BDNF to check its specificity in *Mus Musculus.*

Mus musculus brain derived neurotrophic factor (Bdnf), transcript variant 4, mRNA
Sequence ID: NM_001048142.1 Length: 4009 Number of Matches: 1

Range 1: 662 to 683 GenBank Graphics   ▼ Next Match ▲ Previous Match

Score	Expect	Identities	Gaps	Strand
44.1 bits(22)	3e-05	22/22(100%)	0/22(0%)	Plus/Minus

```
Query  1    CTCCAAAGGCACTTGACTGCTG  22
            ||||||||||||||||||||||
Sbjct  683  CTCCAAAGGCACTTGACTGCTG  662
```
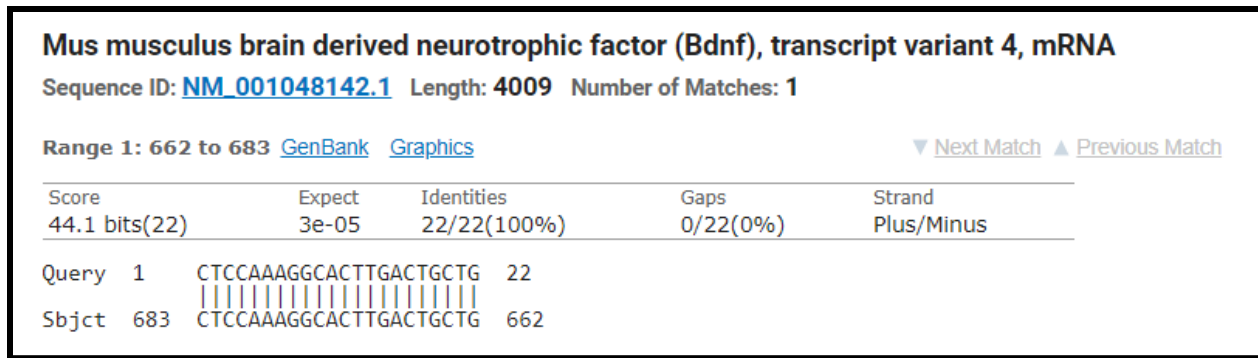
Figure 2.13. BLAST analysis of reverse primer of BDNF. The figure shows the result of nucleotide blast of reverse primer of BDNF to check its specificity in *Mus Muscul*us.

Table 2.2. List of all primers used in this study. This table provides the list of primers along with their sequences, length, GC content and temperatures. It contains comprehensive details to help with understanding and reproducibility of the experimental design.

Name	Primer Sequence	Length	GC%	Optimized annealing temperature °C
BDNF forward	GGCTGACACTTTTGAGCACGTC	22	54.55	64.8
BDNF reverse	CTCCAAAGGCACTTGACTGCTG	22	54.55	64.8
α-synuclein forward	CACTGGCTTTGTCAAGAAGGACC	23	52.17	64.8
α-synuclein reverse	CATAAGCCTCACTGCCAGGATC	22	54.55	64.8
β-actin forward	GCCTTCCTTCTTGGGTATGG	20	55.00	61.5
β-actin reverse	CAGCTCAGTAACAGTCCGC	19	57.89	61.5

2.11.1.5 Amplicon size of BDNF primers

The target genes' known sequences were used to calculate the amplicon size for each set of primers. The forward and reverse primer locations and distances were determined using a reference genomic sequence to determine the anticipated sizes of the PCR products. Comparing the observed band widths with a molecular weight ladder after running the PCR results on an agarose gel

allowed us to validate these calculations. For the PCR amplification process to be accurate and the specificity of the primers to be confirmed, the predicted amplicon sizes are essential.

Range of forward primer = 551 to 572

Range of reverse primer = 662 to 683

Amplicon Size = 683 – 551 + 1

Amplicon Size: 133bp

2.11.1.6 Amplicon size of α-synuclein primers

To guarantee precision and specificity of the PCR results, the process used for BDNF primers was repeated to determine the amplicon size for primers of α-synuclein.

Range of forward primer = 580 to 602

Range of reverse primer = 662 to 683

Amplicon Size = 683 – 580 + 1

Amplicon Size: 104bp

2.11.2 Gradient PCR

The annealing temperature for the chosen primers was optimized by using gradient PCR (Multigene Optimax). We prepared the cDNA and added the components listed in table 2.2. The annealing temperatures were set to 60°C, 62°C, 63.2°C, 64.8°C, 66.4°C and 68°C for the six blocks of the gradient PCR. The PCR protocol included an initial denaturation step at 94°C for 3 minutes, followed by 35 cycles of 94°C for 30 seconds. The annealing temperatures were tested across 40 cycles for each temperature. After PCR, the resulting products were analyzed using gel electrophoresis to check for the presence of bands.

Table 2.3. List of ingredients used in gradient PCR. This table provides a list of all components utilized in gradient PCR along with their quantities.

	Components	Quantity (μl)
1.	cDNA template	2.0
2.	Forward primer	1.0
3.	Reverse primer	1.0
4.	PCR master mix	12.5
5.	Nuclease free water	8.5

2.11.3 Gel electrophoresis

To confirm whether annealing occurred at the correct temperatures, we performed gel electrophoresis using 2% agarose and 10X TBE buffer. We compared the band positions to a DNA ladder ranging from 100 to 1500 bp to determine if annealing was successful. The gels were then analyzed using a Benchtop 2UV transilluminator (LM-20 | P/N 95044902, UVP Co., USA).

2.11.4 Real-Time PCR

Real-Time PCR was used to measure BDNF and α-synuclein expression levels in brain tissues using a Bio-Rad real-time PCR detection system. Mouse β-actin was used as a control with its own primers for qPCR. The reaction mixture was prepared with WizPure™ qPCR Master (SYBR) and included the components listed in table 2.3. The thermocycling settings were as follows: initial denaturation at 94°C for 3 minutes, followed by a second denaturation at 94°C for 30 seconds, then 35 cycles of 30 seconds at 64.8°C, 45 seconds at 72°C, and a final extension at 72°C for 7 minutes. The quality of the PCR product was assessed using amplification curves and agarose gel electrophoresis. The ΔCt values were used to analyze gene expression, normalized against the β-actin values.

2.12 Statistical analysis

Statistical analysis was used to compare the control, MPTP-treated, and CDCA-treated groups to determine if there were significant differences between them. Data were evaluated using one-way

ANOVA followed by Tukey's post hoc test (GraphPad Prism 5.0). Results are presented as mean ± SEM, with a significance level set at $p < 0.05$.
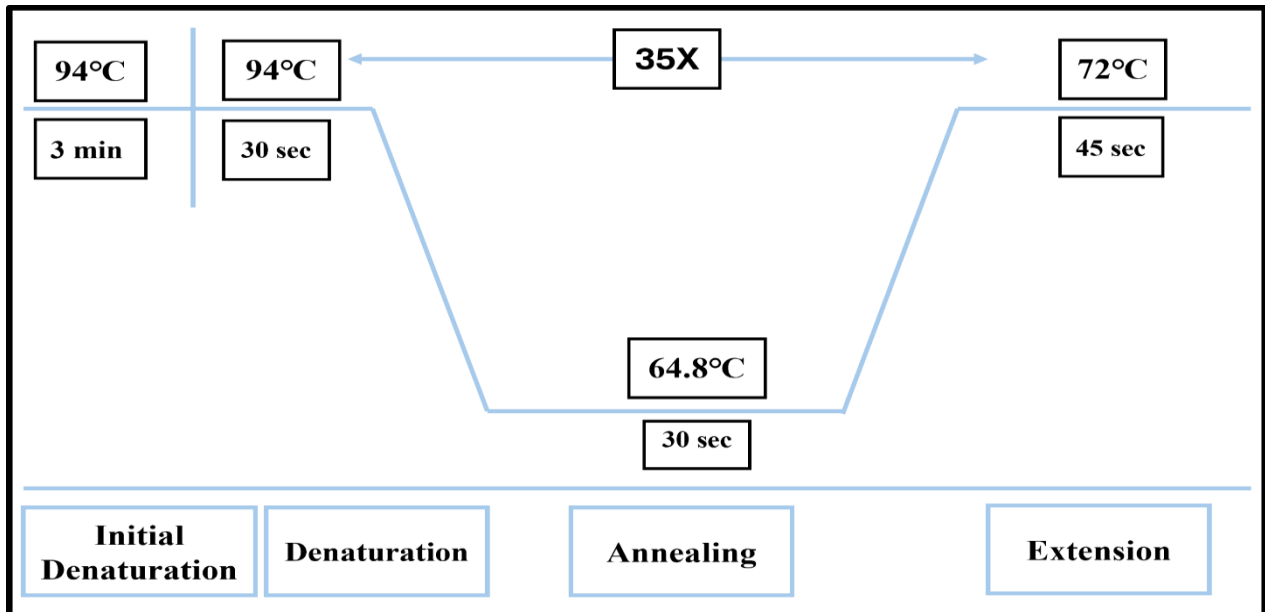
Figure 2.14. Cycling parameters for RT-PCR. The figure shows the thermal cycling profile for both BDNF and α-synuclein.

Table 2.4. List of ingredients used in qPCR. This table provides the list of components of qPCR master mix along with their quantities.

	Components	Quantity (µl)
1.	cDNA template	1.0
2.	Forward primer	1.0
3.	Reverse primer	1.0
4.	SYBR green master mix	4.0
5.	Nuclease free water	13.0

CHAPTER 3: RESULTS

3.1 Results of *in silico* analysis

3.1.1 Structures of Proteins and Ligand

The protein structures of BDNF and α-synuclein, downloaded in PDB format from Alphafold, displaying their 3D shapes. The chemical structure of the ligand, CDCA, is obtained from PubChem in SDF format, providing details about its composition and confirmation. The structures of both the proteins and ligands, shown below in figure 3.1, were then refined and set to publication quality in Discovery Studio Visualizer. These structures are used for further analysis such as molecular docking.
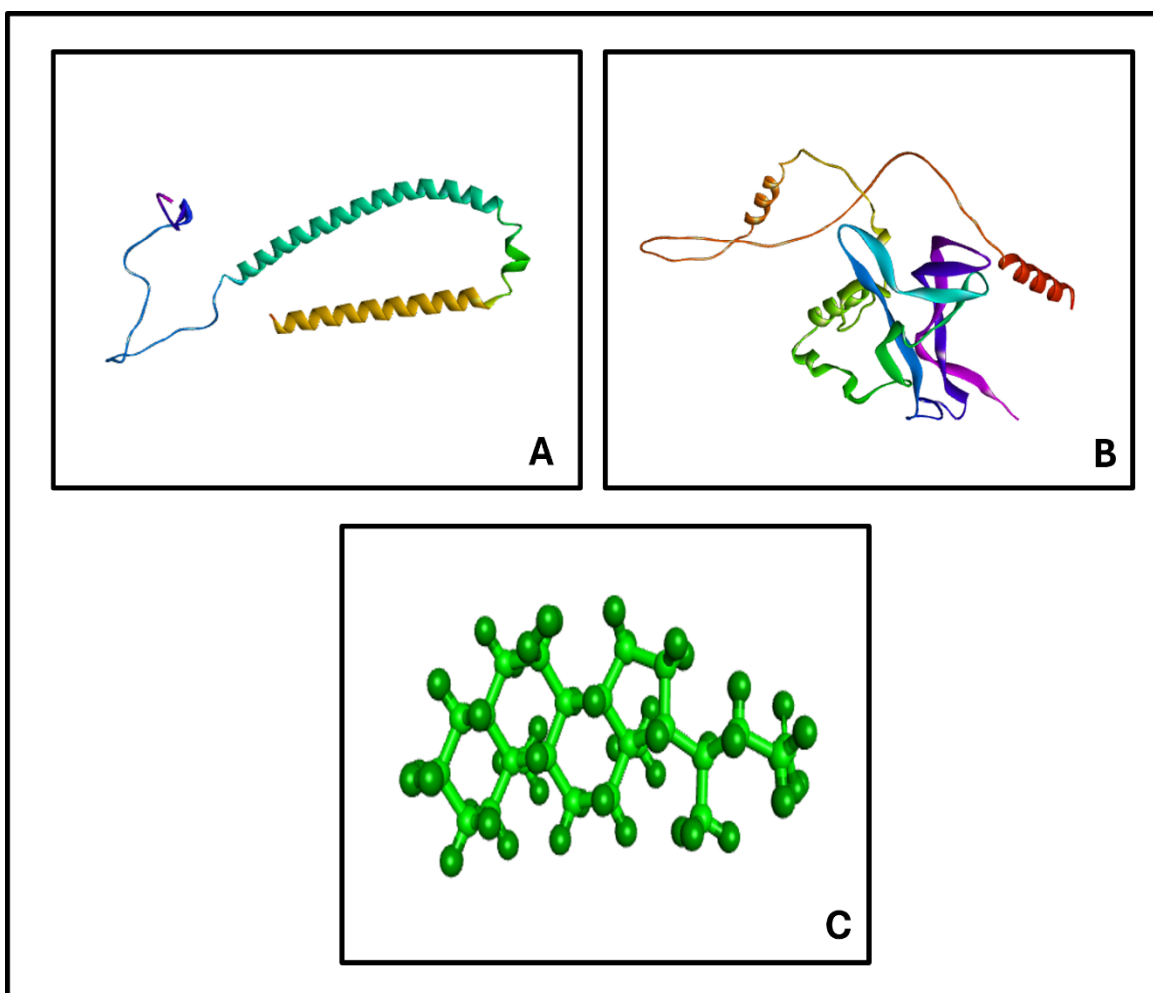
Figure 3.1. 3D structures. The figure presents the three-dimensional (3D) structure of proteins, α-synuclein (A), BDNF (B), and ligand, CDCA (C).

3.1.2 Molecular docking analysis

BDNF and α-synuclein (targets) with CDCA (ligand) were analyzed individually using a ligand-target docking technique. The results show key details about how BDNF and α-synuclein bind with CDCA. This helps understand CDCA's interaction with α-synuclein and BDNF, its role in neuroprotection, and suggests future research directions.
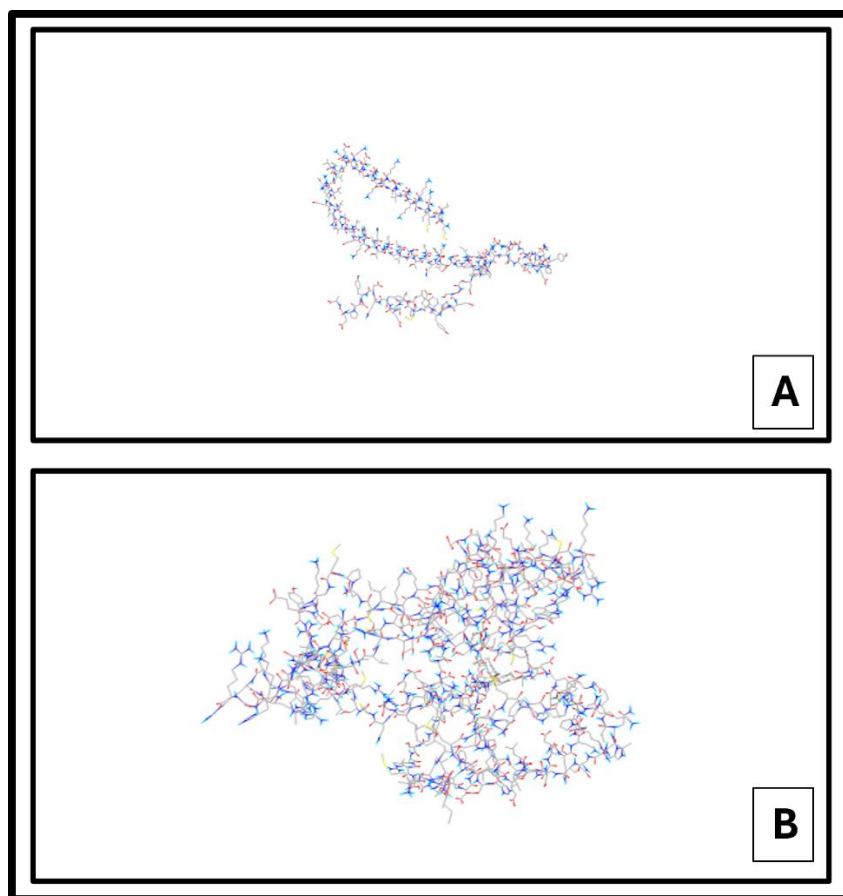
Figure 3.2 Visuals of docking interactions of CDCA, α-synuclein and BDNF. This is a computational representation of the interactions between CDCA and α-synuclein (A) and CDCA and BDNF (B). The representation was derived using a docking analysis performed using PyRx.

3.1.3 Binding affinity

The graphs in Figures 3.3 display the minimal binding energy, showing that CDCA interacted successfully with the target proteins BDNF and α-synuclein. The vertical axis shows the binding affinities between CDCA and the proteins, which are given in energy units (e.g., kcal/mol). Every point on both graphs represents a different computer simulation of docking or binding. Stronger

binding affinities of CDCA to the target proteins are indicated by lower values on the y-axis, indicating a positive interaction. Conversely, lower binding affinity is indicated by higher values. This information contributes to a better understanding of CDCA's potential as a ligand for BDNF and α-synuclein, as well as the stability of the ligand-protein complex and its potential biological implications on neuroprotection.
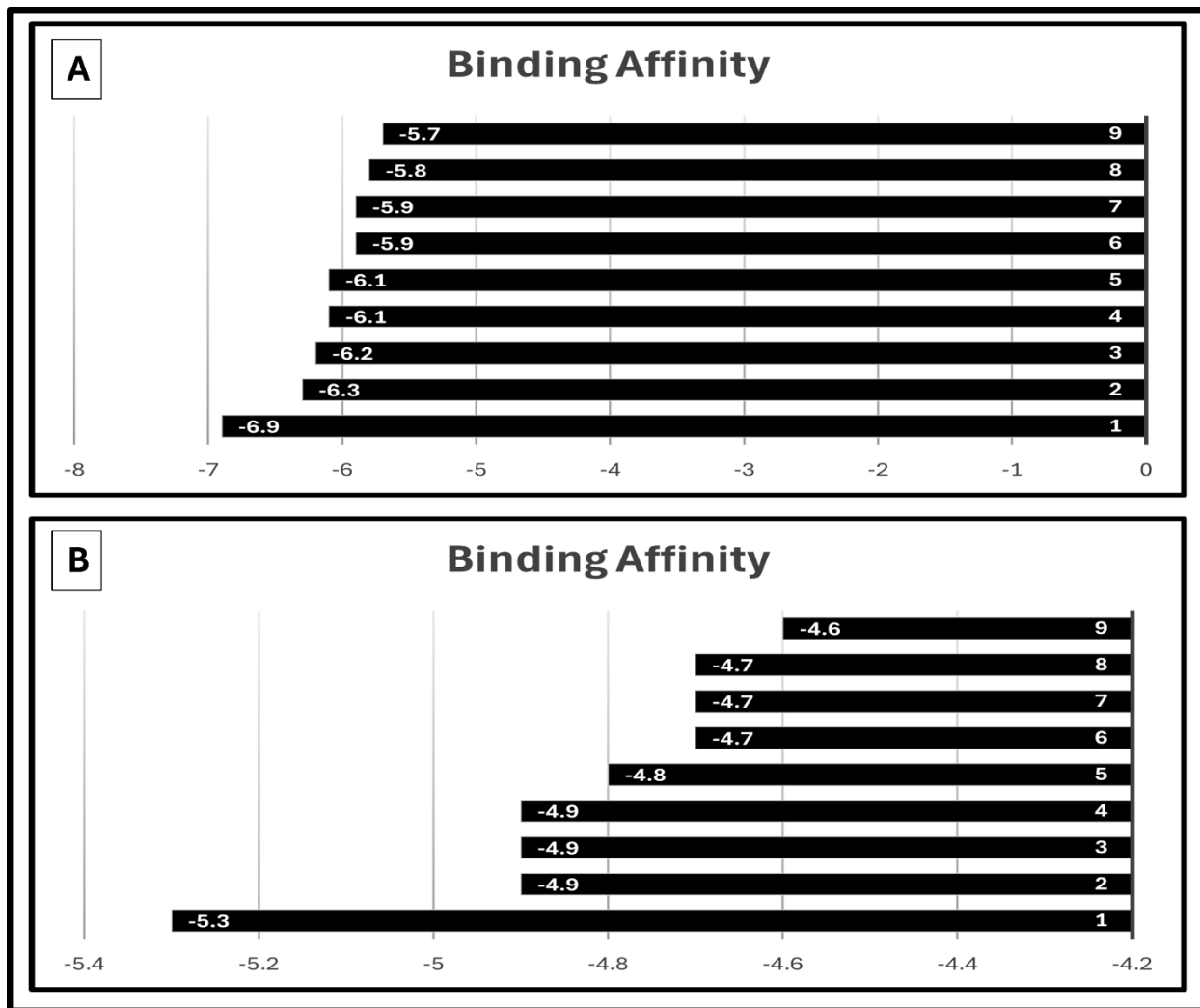
Figure 3.3. Binding energies from docking simulations. *In silico* analysis shows the interaction of CDCA with BDNF, with binding energies that range between – 5.7 to – 6.9 kcal/mol and the average binding energy is **-6.1 kcal/mol** (A). The interaction of CDCA with α-synuclein, with binding energies that range between – 4.6 to – 5.3 kcal/mol and the average binding energy is **-4.8 kcal/mol** (B).
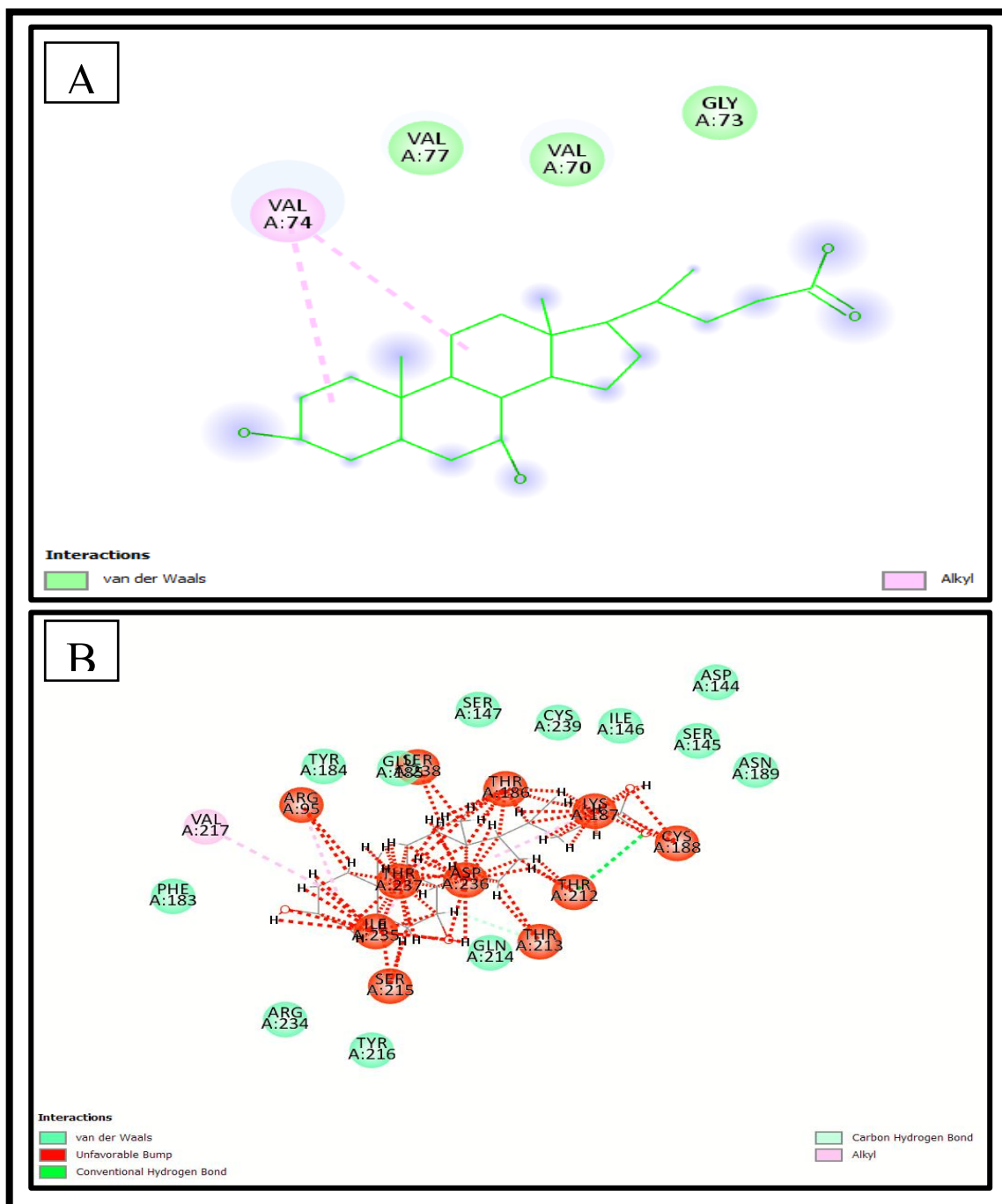
Figure 3.4: The possible locations where α-synuclein and BDNF can bind. Figure A shows the amino acid residues VAL 77, VAL 70, and GLY 73 of α-synuclein engage in Van Der Waals interactions, while VAL 74 forms an alkyl bond. In Figure B the amino acid VAL 217 of BDNF makes an alkyl bond, TYR 216, TYR 184, ARG 234, PHE 183, SER 147, CYS 239, ILE 146, SER 145, ASP 144, ASN 189 play roles in creation of Vander Waals Interactions and THR 21 makes conventional hydrogen bond.

3.2 Behavioral assessment results after disease induction with MPTP

3.2.1 Open field test

Figure 3.5 illustrates how behavior affected the open field test. There were six mice in each group. The test examined the number of entries in the peripheral and central region. Using the T-test, the results demonstrated a significant difference between groups I (Control) and II (MPTP), indicating that the diseased animals had less entries in the central region, however, the animals in the control group were more likely to spend time in the central region and had more entries to it.
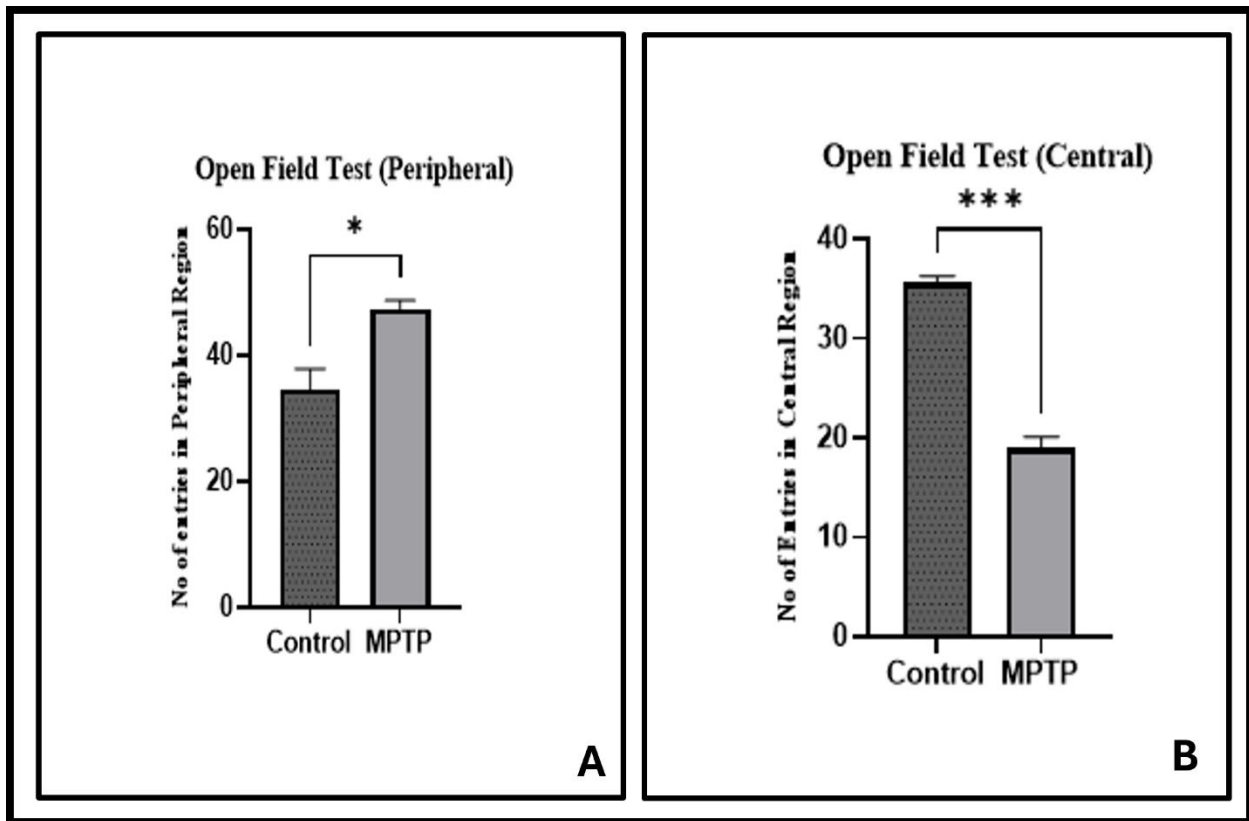
Figure 3.5 Open Field Test after the administration of MPTP. Graph A and B show the no entries of control and MPTP group in central and peripheral area. Comparison between control and MPTP group was done by using T test. Data is presented as mean ± SEM. *p<0.05, ***p<0.001.

3.2.2 Tail suspension test

Figure 3.6 illustrates how MPTP affects the tail suspension test. There were six mice in each group. The parameter we evaluated in the test was the immobility time. Using the T-test, it was discovered

that control group and MPTP-treated group differed significantly from one another and it showed that group II receiving MPTP experienced longer periods of immobility.
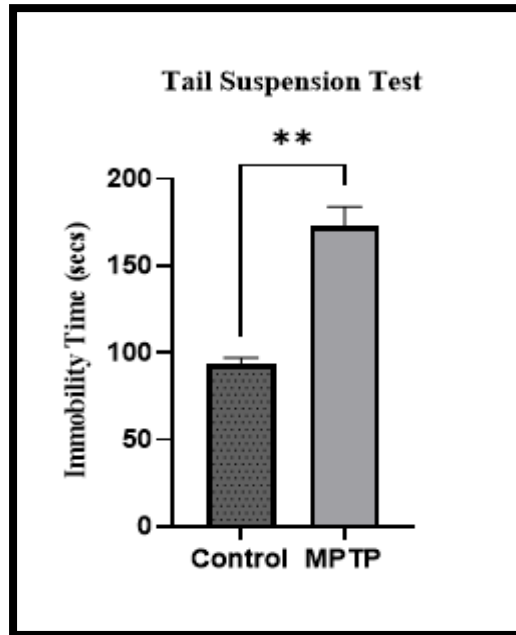
Figure 3.6 Tail suspension test after the administration of MPTP. The graph shows the immobility time of control and MPTP group. Comparison between control and MPTP group was done by using T test. Data is presented as mean ± SEM. **$p<0.01$.

3.3 Behavioral assessment results after treatment with CDCA

3.3.1 CDCA ameliorates anxiety like and exploratory behavior in PD mouse model

One popular method for evaluating behavioral changes after MPTP treatment is the open-field test. Typically, diseased mice spend more time near the periphery of the field and make fewer entries into the center compared to healthy ones. The results show the effect of MPTP and CDCA administration on the anxiety like and exploratory behavior of mice. Mice in the MPTP group had an increased anxiety level and less exploratory activity in the central region, while those treated with CDCA showed a significant decrease in anxiety level (figure 3.7). Overall, the open field test demonstrates that CDCA can reduce the behavioral deficits caused by MPTP and help restore normal behavior in treated mice.
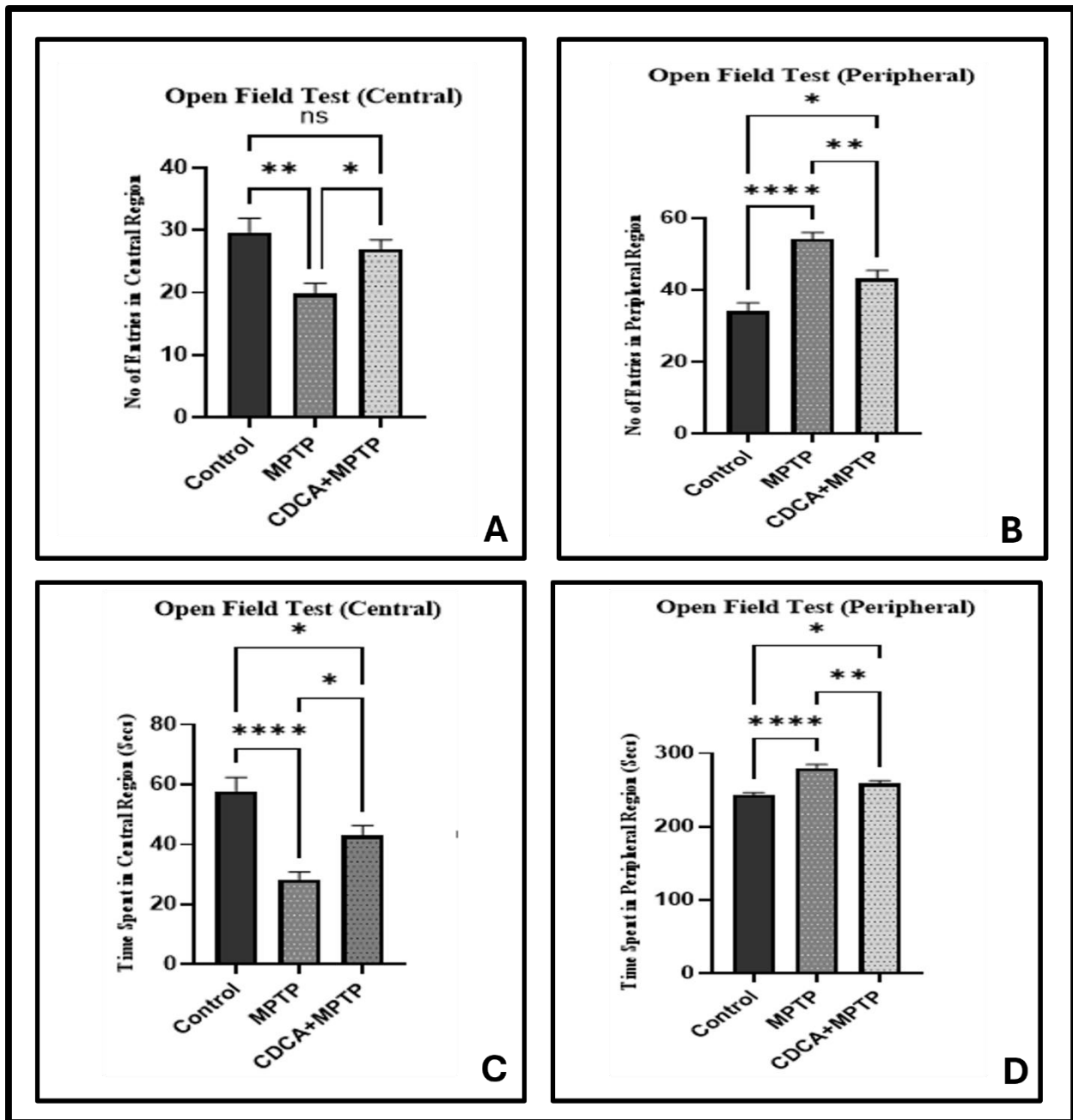
Figure 3.7 Open filed test after the administration of CDCA. Graph A and B show the no entries of control, MPTP and CDCA+MPTP group in central and peripheral region whereas the graphs C and D show the time spent in central and peripheral region. Comparison between control, MPTP and CDCA+MPTP group was done by using one-way ANOVA followed by Tukey's post-hoc test. Data is presented as mean ± SEM. ns=non-significant, *p<0.05, **p<0.01, ****p<0.0001.

3.3.2 CDCA demonstrates antidepressant properties in PD mouse models

The tail suspension test and forced swim test were used to assess the antidepressant effects of CDCA on mice. Figure 3.8A illustrates that the mice in the control group were much better at swimming than the group that received MPTP treatment. Conversely, the CDCA treated group displayed less floating time than the MPTP treated group. In contrast to control mice, in tail suspension test, MPTP-treated mice's immobility duration was considerably longer (figure 3.8B), and the CDCA group's mice were more frequently mobilized than the mice of MPTP treated group. The collective outcomes of the two experiments indicate that CDCA can help treated mice return to their normal behavior by suppressing MPTP-induced depression-like behavior.
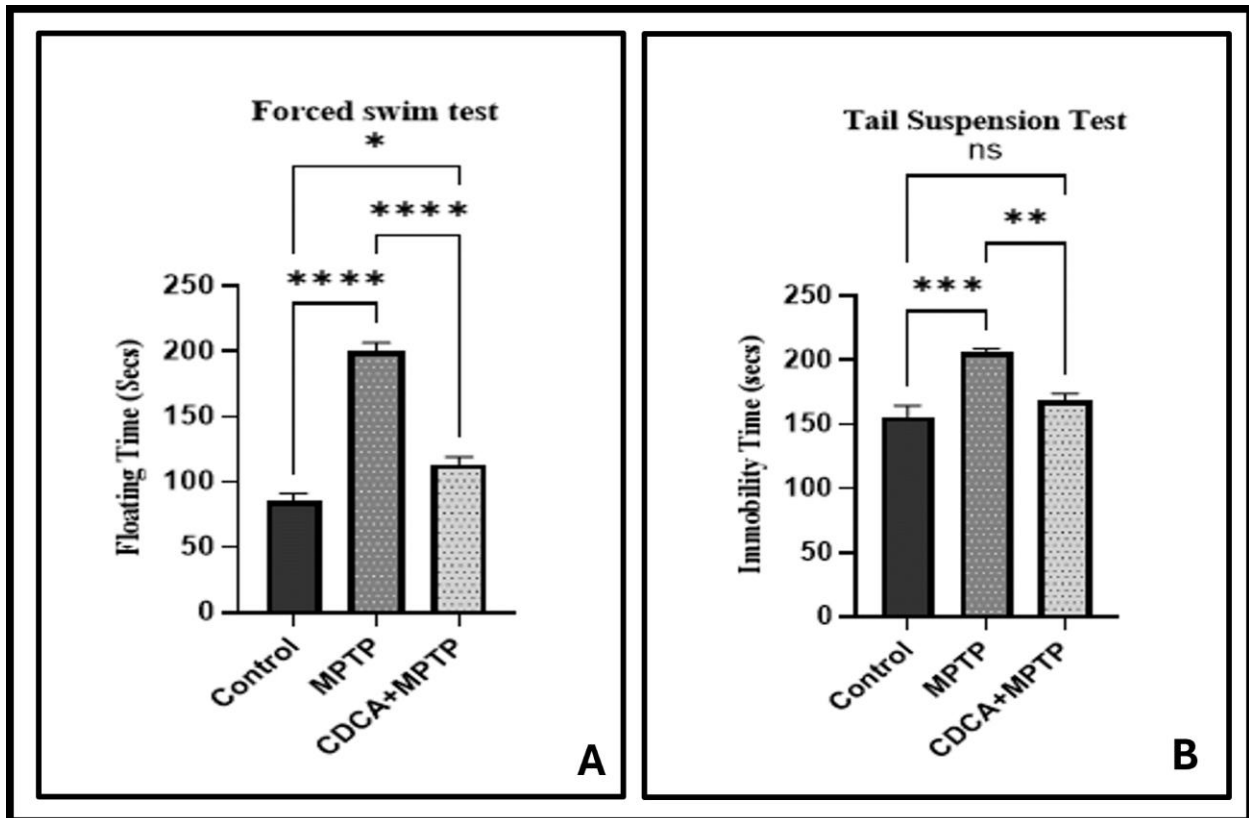
Figure 3.8 Forced swim and tail suspension test after the administration of CDCA. Graph A shows the floating time of control, MPTP-treated and CDCA-treated groups. While graph B shows the immobility time of control, MPTP-treated and CDCA-treated groups. Comparison among these three groups was done by using one-way ANOVA followed by Tukey's post-hoc test. Data is presented as mean ± SEM. ns=non-significant, *p<0.05, **p<0.01, ***p<0.001, ****p<0.0001.

3.3.3 CDCA reduces motor impairment and enhances spatial working memory in PD mouse models

Using the Pole test, the motor abilities of mice in the control, MPTP-treated, and CDCA-treated groups were compared. Turn time was the feature that we measured in the pole test. According to the pole test results, as shown in figure 3.9A, the control group turned faster than the MPTP-treated group, and when the CDCA-treated group was compared to the MPTP-treated group, the CDCA-treated group turned faster. The Y maze test was to assess how CDCA therapy affected the impaired spatial working memory caused by MPTP. Figure 3.9B demonstrates that the MPTP-treated group had a decrease in the percentage of spontaneous alternations, whereas the control group displayed a much larger percentage of alternations than the other two groups. However, compared to the MPTP-treated group, the CDCA-treated group displayed a noticeably higher percentage of alternation. These results suggest that CDCA improves motor performance as well as cognitive function.
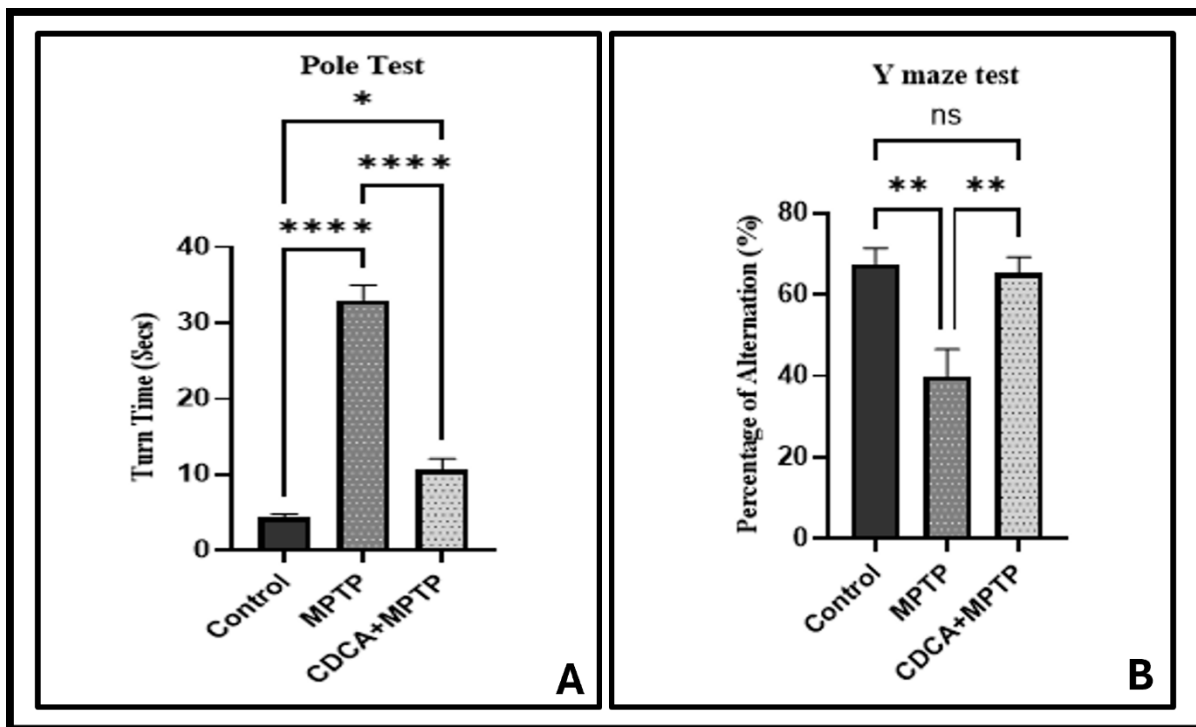
Figure 3.9 Pole and Y maze Test after the administration of CDCA. Graph A shows the turn time of control, MPTP-treated and CDCA-treated groups. While graph B shows the percentage of alternations of control, MPTP-treated and CDCA-treated groups. Comparison among these

three groups was done by using one-way ANOVA followed by Tukey's post-hoc test. Data is presented as mean ± SEM. ns=non-significant, *p<0.05, **p<0.01, ****p<0.0001.

3.4 Histopathological results

3.4.1 CDCA's neuroprotective properties against MPTP-induced neurodegeneration

The midbrain, cerebellum, cortex and hippocampal histological structures are all normal in the control group, nevertheless, exposure to MPTP caused substantial neuronal degeneration in each of these brain regions. However, the histological traits improved in the group that received CDCA treatment. The cells in the MPTP-treated areas of the midbrain, cortex, cerebellum, and hippocampus are shrunken, have formed clusters in certain locations, and have an irregular, elongated shape; in contrast, the cells in the control group are spherical and regular in shape. By CDCA, the damage was prevented. As far as the cell count is concerned, the number of cells showed a marked decrease in the MPTP-treated group. However, treatment with CDCA prevented degeneration, indicating its potential neuroprotective effect.

3.4.1.1 Midbrain

Through histological staining with H&E and subsequent analysis, the effect of CDCA on the midbrain of mice treated with MPTP was evaluated. Figure 3.10 (A, B, C) provides a visual illustration of coronal sections of midbrain. Normal neuronal cells with a noticeable nucleus were visible in the control midbrain. Observations from the MPTP-treated group's midbrain revealed higher indications of irregularly shaped and shrunken cells as well as neuronal degeneration with a reduction in the number of neurons. On the other hand, there were less deteriorated neurons and more normal neurons in the CDCA-treated group. Additionally, cell counting was carried out on digital photomicrographs using Image J software and the results in Figure 3.10D show that the MPTP administration caused significant loss of dopaminergic neurons while the group treated with CDCA has a greater number of neurons as compared to MPTP- treated group.

3.4.1.2 Cerebellum

Sections of the control mouse's cerebellum stained with H&E revealed the normal histological structure of the cerebellum. The MPTP-treated group's cerebellar Purkinje cell is not in uniform shape than those of the control group's. On the other hand, Purkinje cell size and shape improved in the CDCA-treated group (Figure 3.11). Additionally, the cell count demonstrates that the

MPTP-treated group had significantly less cells in the section of cerebellum, whereas the CDCA-treated group had more cells
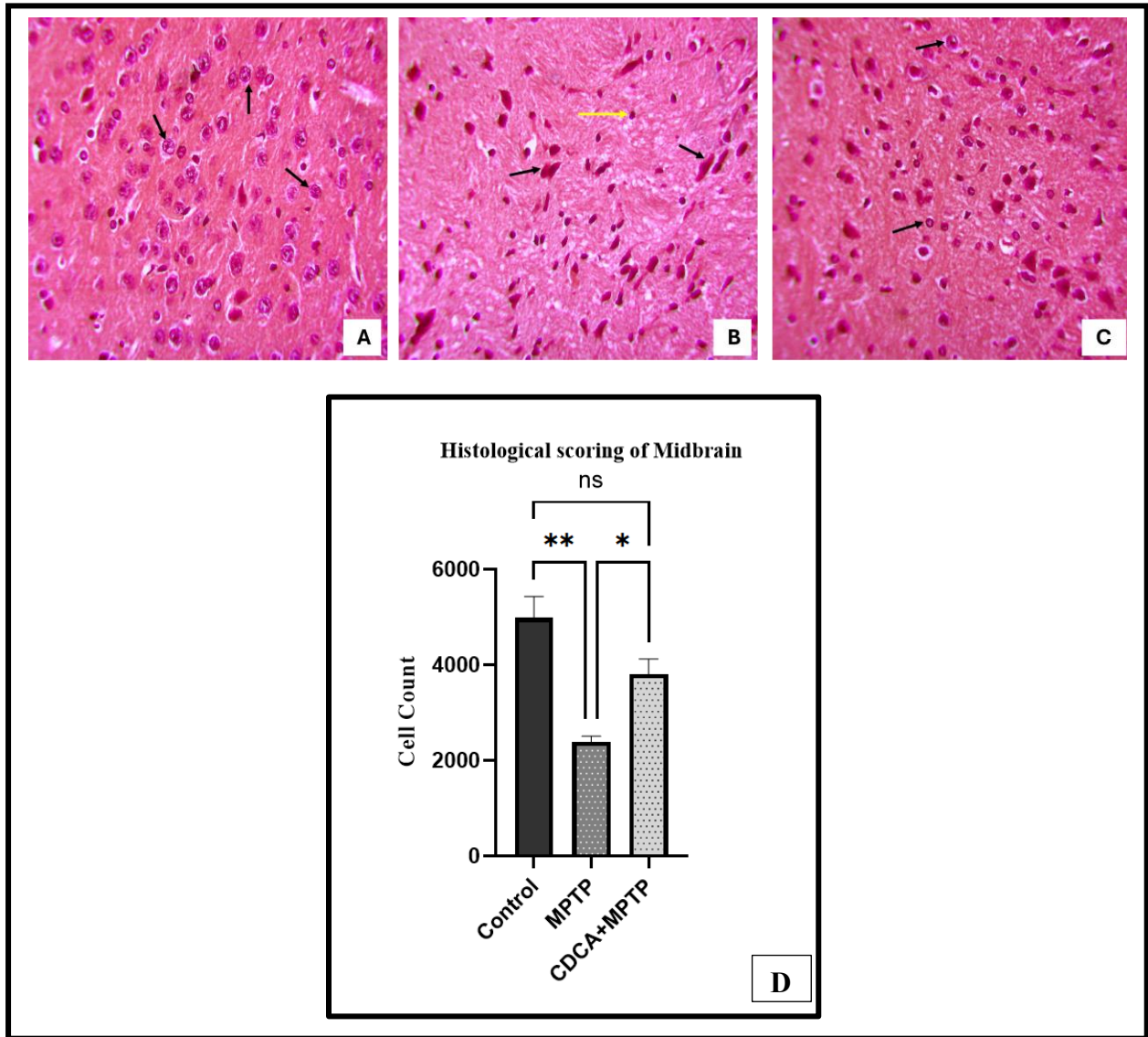
Figure 3.10 The section of the coronal midbrain stained with H&E (40X) and the histological scoring. The figure shows the photomicrographs in which the arrows in the control group show intact, uniform and round shaped cells (A). The black arrows in MPTP-treated group show elongated and irregular shaped cells, yellow arrow shows shrunken cells while the arrow heads show the cluster of cells (B). The histological features of CDCA-treated group are better and there are significantly a smaller number of irregular shaped cells, and the arrows indicate the presence of the round shaped cells (C). On the other hand, the graph in this figure shows cell count of three groups (D). Comparison among these three groups was done by using one-way

ANOVA followed by Tukey's post-hoc test. Data is presented as mean ± SEM. ns=non-significant, *p<0.05, **p<0.01.
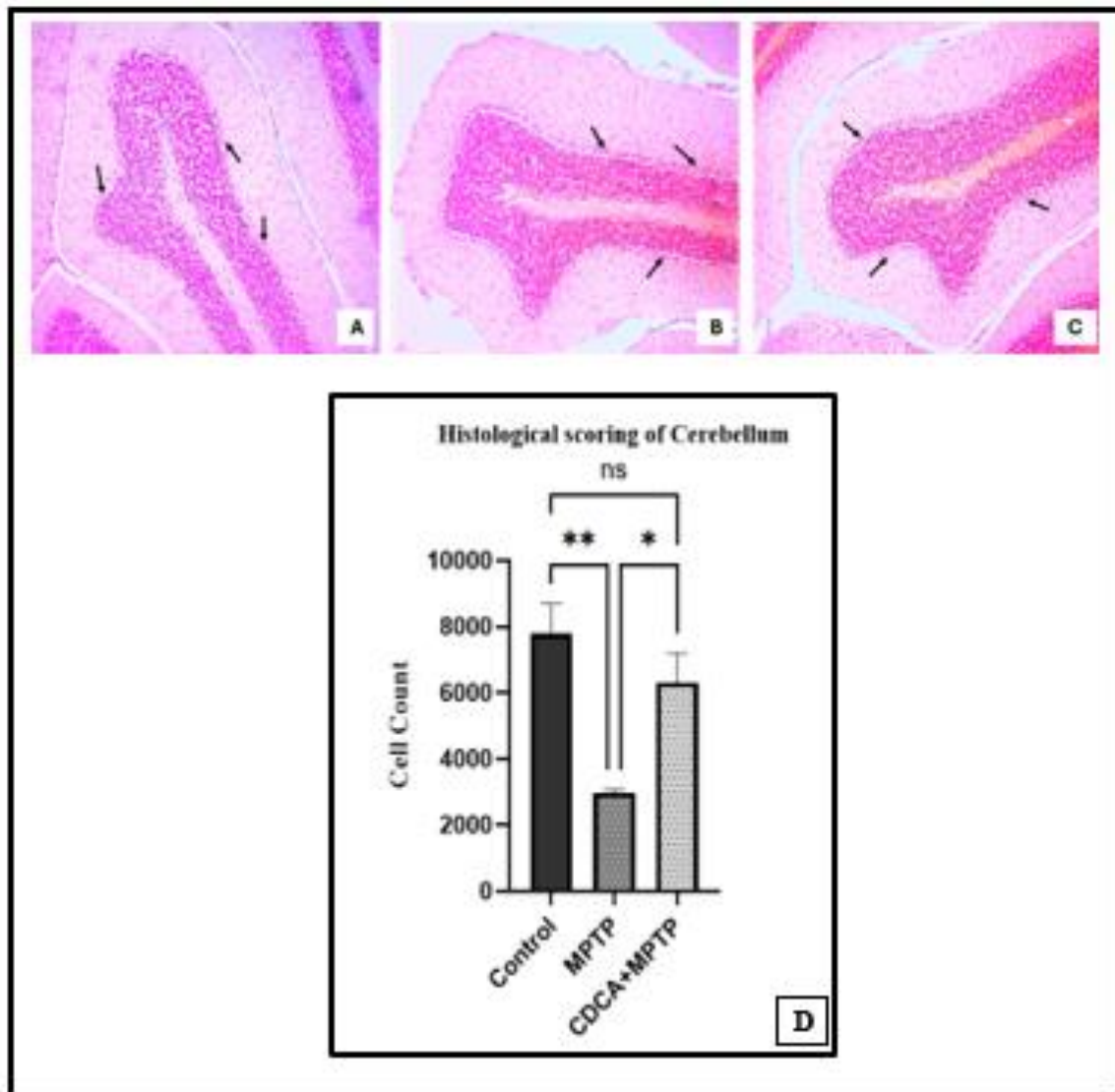
Figure 3.11 The section of the Cerebellum stained with H&E (10X) and the histological scoring. The figure shows the photomicrographs of cerebellum in which the arrows in the control group show intact, uniform and round Purkinje cells (A). The arrows in MPTP-treated group show elongated and shrunken Purkinje cells (B). The histological features of Purkinje cells of CDCA-treated group are better as shown by arrows and there are significantly a smaller number of irregular shaped cells and more well-defined cells (C). On the other hand, the graph in this figure shows cell count of three groups (D). Comparison among these three groups was done by using

one-way ANOVA followed by Tukey's post-hoc test. Data is presented as mean ± SEM. ns=non-significant, *p<0.05, **p<0.01.

3.4.1.3 Cortex

The cortex (Figure 3.12) in the brain of control mice showed normal histological architecture and undamaged neurons under a microscope. Conversely, the MPTP-treated group's cells exhibited enlarged intracellular gaps, irregular shapes, and disorganized structures, all of which point to cell tissue deterioration. Moreover, we observe blood vessel congestion and cell shrinkage because of MPTP. In the meanwhile, animals given CDCA showed typical histological characteristics in their cortex, with a greater number of round cells and very few degenerated cells. Furthermore, the histological scoring carried out using Graph Pad prism demonstrates that the MPTP-treated group had fewer cells overall because of decreased cell density and greater intercellular spacing and when we compare this group to the CDCA-treated group, we can observe that the CDCA has a higher cell density and therefore more cells.

3.4.1.4 Hippocampus

A section of the brain stained with H&E is shown in Figure 3.13, which highlights the histological features of the hippocampal tissue. The control group's tissue structure was healthy and well-preserved, and no histological alterations were seen. The cells also showed normal morphology. Conversely, the MPTP-treated group's hippocampus showed shrunken pyramidal cells and upon examination of the hippocampal pyramidal layer of the CDCA-treated group, normal neurons were seen. Furthermore, the number of pyramidal cells in the hippocampal section shows that the MPTP-treated group had substantially fewer pyramidal cells than the CDCA-treated group.

3.5 Results of PCR

3.5.1 Gradient PCR results

The results of the gel electrophoresis show that gene-specific primers were used to amplify the mRNA for BDNF and α-synuclein (figure 3.14). With incremental temperature adjustments of 2°C, the bands were detected over a gradient of 60°C to 68°C. After gel electrophoresis, many bands were visible, matching the predicted sizes of BDNF at 133 base pairs and α-synuclein at 104 base pairs as shown in figure 3.14. Nevertheless, certain bands were poorly defined and showed signs of primer-dimers or non-specific amplification. We chose a temperature that resulted in a
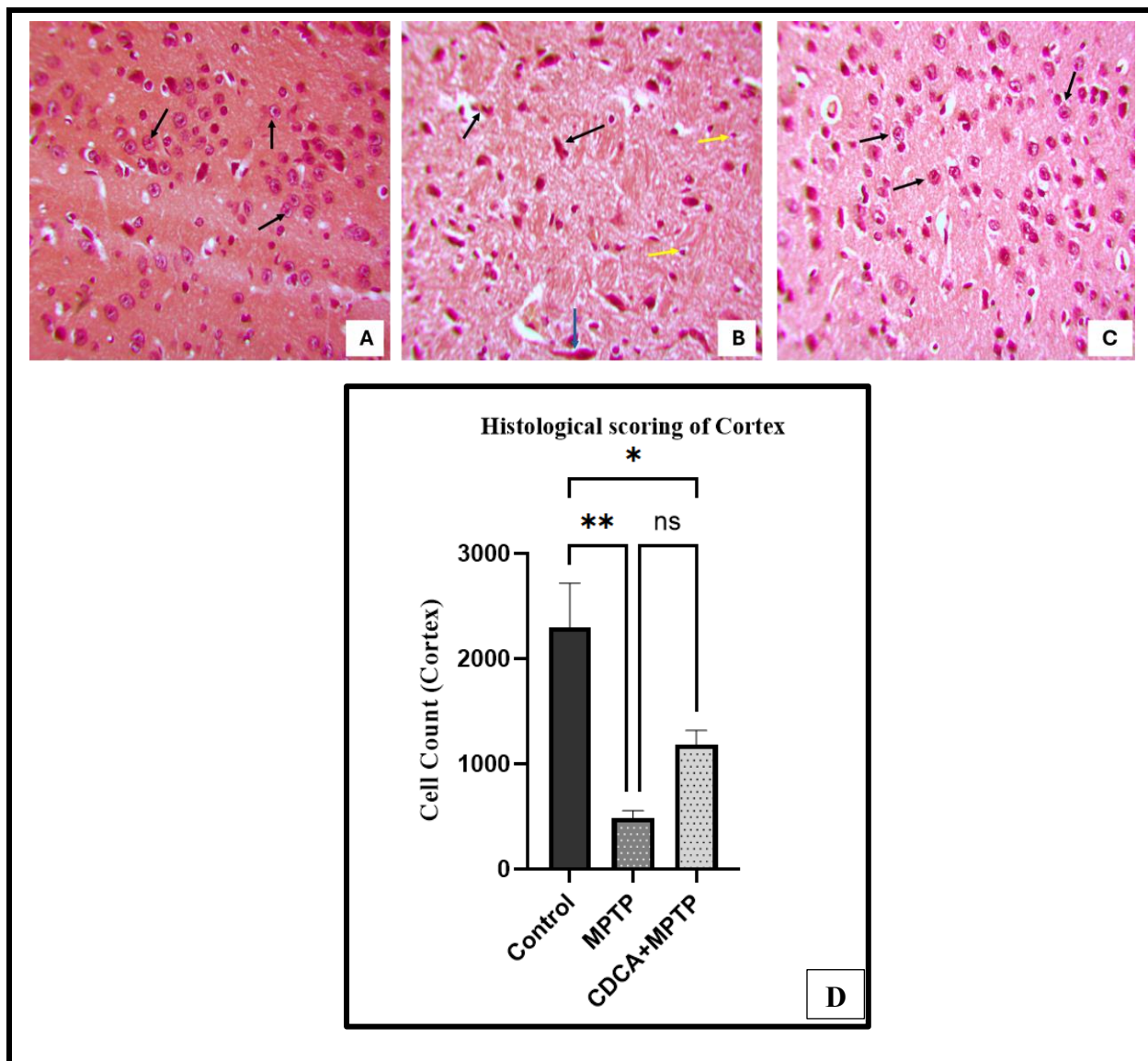
Figure 3.12 The section of the cortex stained with H&E (40X) and the histological scoring.

The figure shows the photomicrographs in which the cortex in the control group shows no histopathological changes (A). The black arrows in the MPTP-treated group show degenerated and irregular shaped cells, while the yellow arrows show shrunken neurons, and the blue arrow shows mild congestion of blood vessels (B). Sections from the group treated with CDCA show normal neurons and less degeneration(C). On the other hand, the graph in this figure shows cell count of three groups (D). Comparison among these three groups was done by using one-way ANOVA followed by Tukey's post-hoc test. Data is presented as mean ± SEM. ns=non-significant, *p<0.05, **p<0.01.
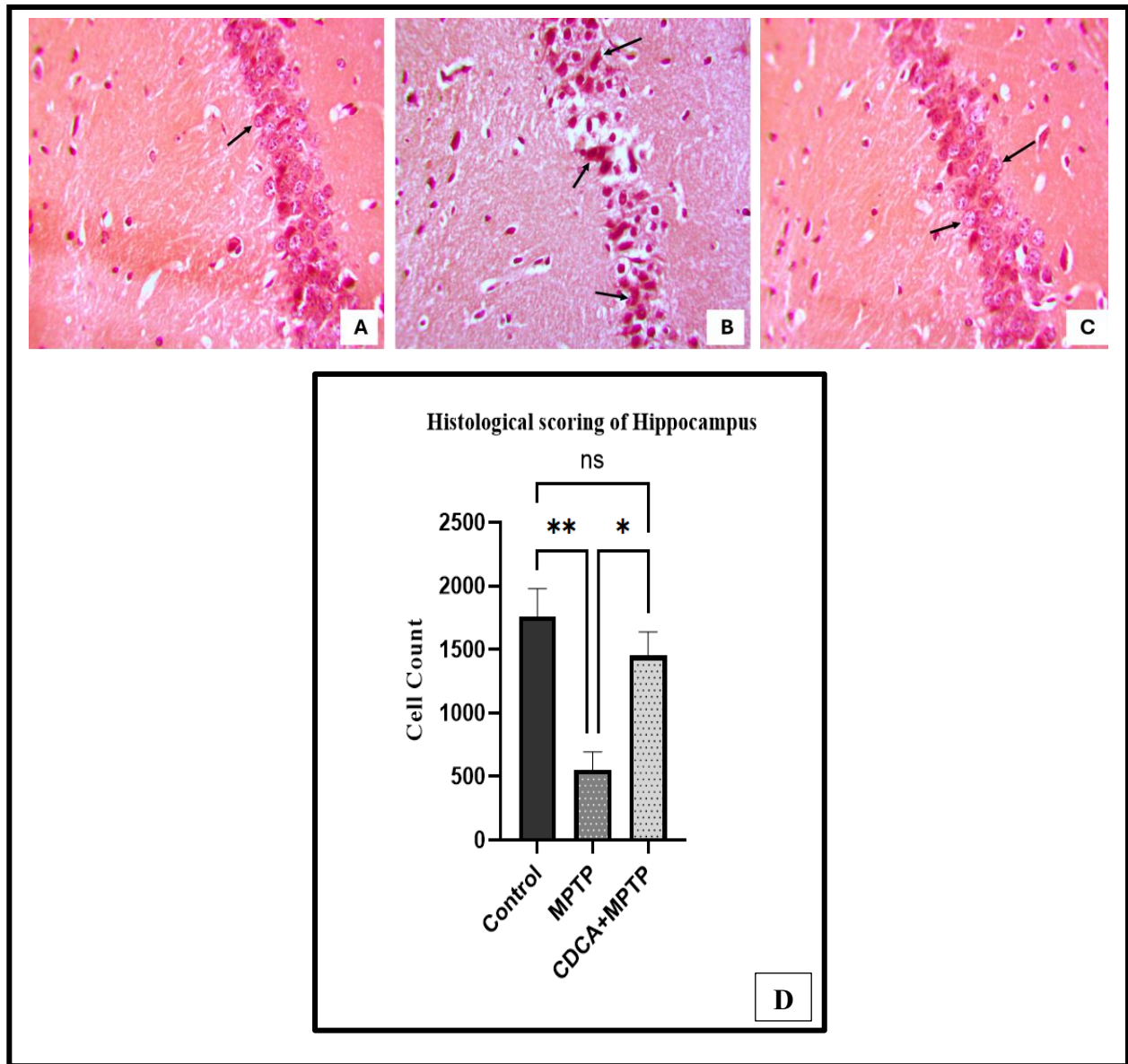
Figure 3.13 The section of the hippocampus stained with H&E (40X) and the histological scoring. In the hippocampal layer of the control group, normal neurons were visible (A). Numerous degenerating neurons were visible in the pyramidal layer of the MPTP-treated group, as indicated by the arrows (B). The arrows in section from CDCA-treated group showed normal pyramidal neurons (C). On the other hand, the graph in this figure shows cell count of three groups (D). Comparison among these three groups was done by using one-way ANOVA followed by Tukey's post-hoc test. Data is presented as mean ± SEM. ns=non-significant, *$p<0.05$, **$p<0.01$.

distinct band devoid of any dimers or non-specific bands. For both primers, the ideal temperature was 64.8°C since at this temperature, each of them produced unique bands. Crucially, this temperature choice fulfils two functions by matching the overlapping temperature ranges for both α-synuclein and BDNF. This optimization provides valuable information on the brain-related expression patterns of these genes and makes the PCR amplification more precise and sets the basis for further molecular analysis by guaranteeing the specificity of the PCR amplification.
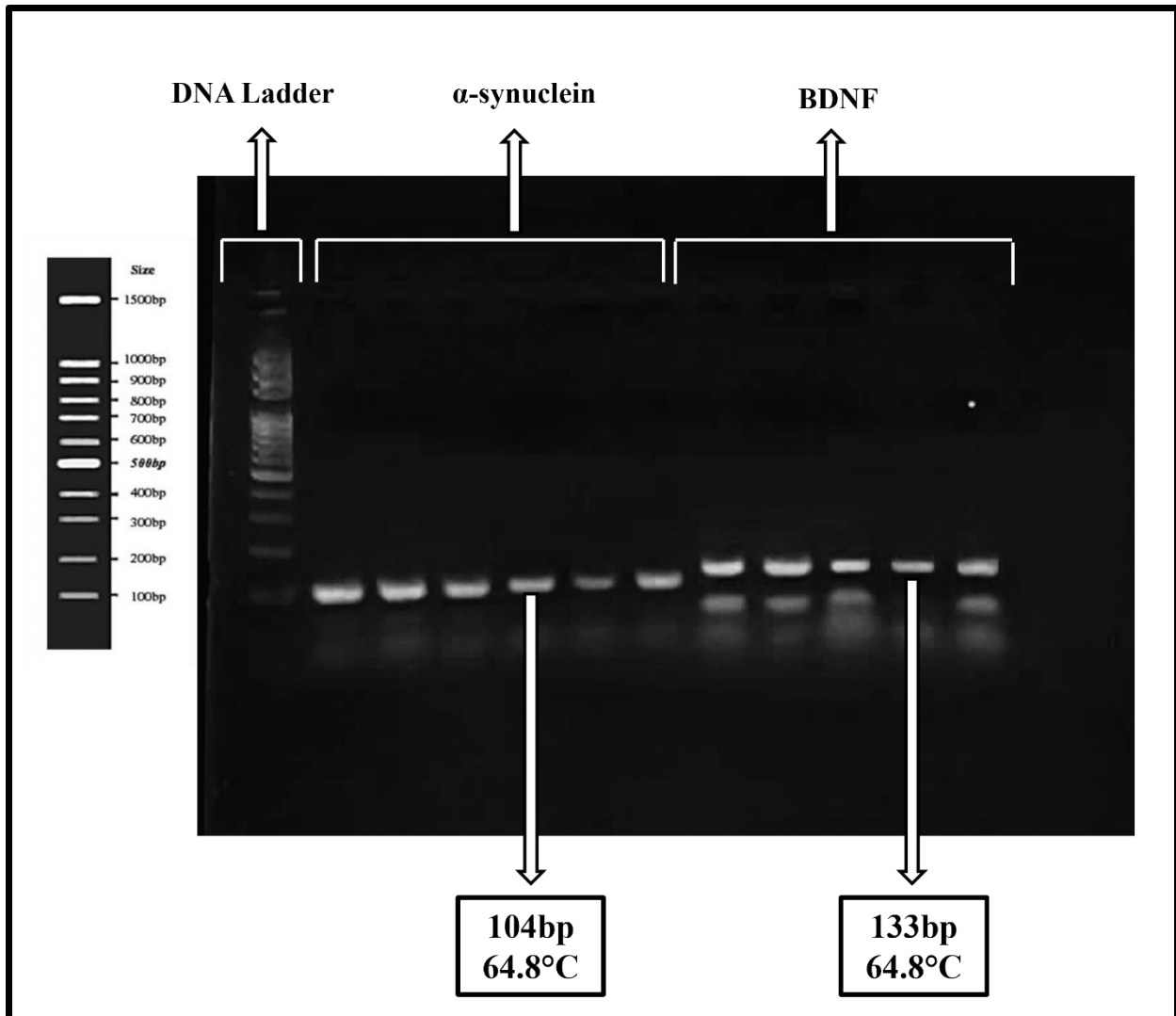
Figure 3.14. Gel electrophoresis results of gradient PCR for primer optimization. α-synuclein and BDNF were the two specific genes whose expression was to be evaluated by gradient PCR study on the mouse brain. There are clearly visible bands in the resulting gel electrophoresis that match the predicted sizes of the amplified DNA fragments. Interestingly, a

strong band appears at roughly 104 base pairs, indicating the effective amplification of α-synuclein, at an optimized temperature of 64.8˚C. At the same temperature, bands at 133 base pairs simultaneously appear, suggesting that BDNF was successfully amplified.

3.5.2 Real-Time PCR result

3.5.2.1 CDCA reverses the increase α-synuclein level in PD mouse model

The relative expression level of α-synuclein is shown in figure 3.15. As a housekeeping gene for internal control, ß-actin was used to measure and normalize the expression of α-synuclein during the assessment process. The findings point to a noticeable alteration in the patterns of gene expression. It was discovered that the mice given MPTP exhibited up-regulation of α-synuclein mRNA expression, which is suggestive of the pathophysiology of PD and could also lead to neurodegeneration and Lewy body formation due to α-synuclein buildup. Conversely, α-synuclein was down-regulated after receiving CDCA medication, indicating that CDCA may have a protective effect against the elevated α-synuclein expression linked to PD.
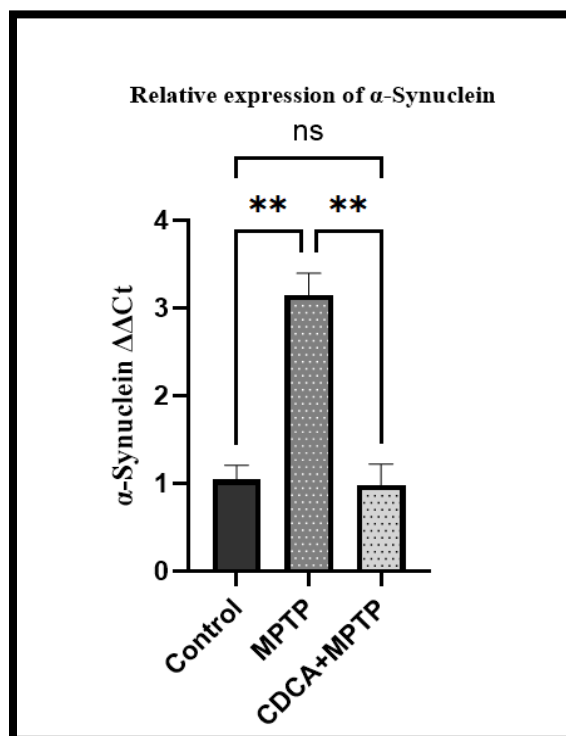
Figure 3.15. The relative expression of α-synuclein mRNA (normalized to β-actin). α-synuclein mRNA expression was shown to be up-regulated in the mice treated with MPTP, but down-regulation was observed in the mice treated with CDCA. Comparison among these three

groups was done by using one-way ANOVA followed by Tukey's post-hoc test. Data is presented as mean ± SEM. ns=non-significant, **p<0.01.

3.5.2.2 CDCA enhances BDNF expression in PD mouse model

The down-regulation of BDNF mRNA expression was seen in the group of mice treated with MPTP, suggesting a reduced level of neuroprotection and neuroplasticity and perhaps increasing neurodegeneration. Interestingly, CDCA treatment caused BDNF mRNA expression to increase as shown in figure 3.16. These results suggest that CDCA may have a regulatory role in counteracting the down-regulation observed in the MPTP-treated group. Regarding the molecular processes associated with PD and the potential modulatory effects of CDCA on BDNF expression, these findings offer significant new insights.
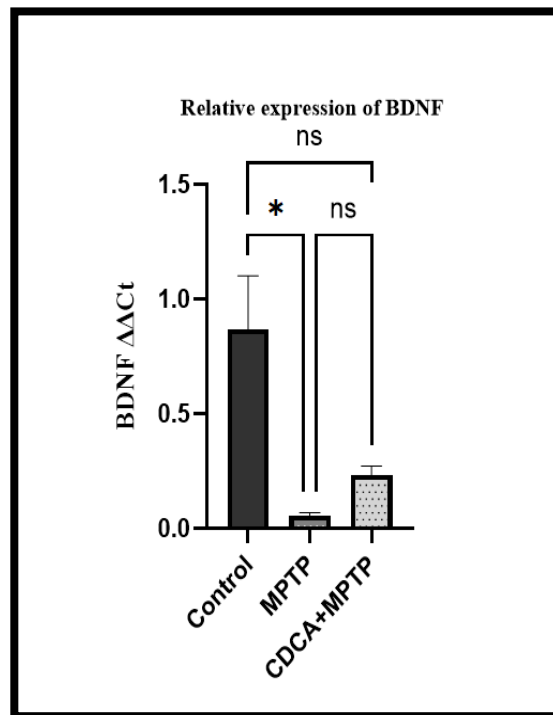
Figure 3.16. The relative expression of BDNF mRNA (normalized to β-actin). In the mice treated with MPTP, BDNF mRNA expression was shown to be down-regulated, whereas the mice treated with CDCA showed up-regulation. Comparison among the three groups was done by using one-way ANOVA followed by Tukey's post-hoc test. Data is presented as mean ± SEM. ns=non-significant, *p<0.05.

CHAPTER 4: DISCUSSION

Worldwide, neurological disorders pose a serious threat to healthcare systems. These diseases are regrettably becoming more common and hurting a lot of individuals because of how stressful life is in the present period. Furthermore, there are little or no therapy options available for many such disorders. Most prescription medications only treat the symptoms of the disease [62]. One of those disorders is PD which is characterized by slow and progressive loss of dopaminergic neurons in the substantia nigra. Loss of dopamine terminals occurs because of this neuronal degeneration not just in the striatum but also in other basal ganglia and cortical brain areas [63]. Recent years have seen significant progress in the treatment of PD, partly due to new understandings of its pathogenesis obtained via the development of animal models of parkinsonism. MPTP exposure has the potential to cause Parkinsonism in humans, nonhuman primates, and some other animals [64]. Numerous research has revealed that using different compounds in rodent models may protect against Parkinsonism. Strategies include: raising neurotrophic factors to promote neuronal survival and inhibit apoptosis and neurodegeneration; blocking the generation of reactive oxygen species; and utilizing chemical chaperones that activate HSP and lessen the ER stress response to increase protein stability within the cell [65]. One of such compounds which enhance neurotrophic factors, reduce neurodegeneration and apoptosis is CDCA, a primary bile acid. BDNF and α-synuclein, two biomarkers that are important in the pathophysiology of PD, were chosen for our study. The results of molecular docking show that CDCA interacts successfully with BDNF and α-synuclein. This suggests that CDCA may have therapeutic implications in PD models. Strong interactions are indicated by the binding affinities, which shed light on the underlying molecular mechanisms.

It has been found by using molecular docking simulations that CDCA binds to BDNF and α-synuclein in a variety of ways, each with a distinct binding affinity. Different conformations and orientations of CDCA inside the binding pocket of both proteins may be the cause of the differences in binding affinities. It is believed that there is a significant connection between CDCA and BDNF as well as between CDCA and α -synuclein by the most favorable binding location, which is evidenced by high negative binding affinities. The binding energies for the interaction between CDCA and BDNF range from -5.7 to -6.9 kcal/mol, with an average of -6.1 kcal. These results point to a strong binding affinity, suggesting that CDCA and BDNF can interact with each other efficiently at the molecular level. Reduced expression of BDNF is linked to

neurodegenerative diseases like PD. BDNF is a crucial neurotrophin involved in neuronal survival, development, and plasticity. The strong binding affinity noted in this interaction suggests that CDCA may regulate BDNF activation, hence amplifying its neuroprotective benefits. This interaction has the potential to boost neuronal survival and improve neuroplasticity, both of which are required to battle the neurodegenerative processes in PD.

The interaction between α-synuclein and CDCA has binding energies that range from -4.6 to -5.3 kcal/mol, with an average of -4.8 kcal/mol. These results show a significant binding affinity even if they are marginally lower than those found for the CDCA-BDNF interaction. α-synuclein is a protein that contributes to PD by aggregating and forming Lewy bodies. Given that CDCA can bind to α-synuclein, it is possible that it will affect how α-synuclein aggregates, which could lessen its toxicity. This might be helpful in reducing the development of Lewy bodies and delaying the onset of PD. These two functions demonstrate CDCA's potential as a PD treatment drug, providing neuroprotective advantages and maybe delaying the progression of the disease.

For the first time, the neuroprotective effects of CDCA in the MPTP/MPP+ models of PD were examined in this study. MPTP is a drug that is frequently used to evaluate new compounds for their neuroprotective qualities and to generate a Parkinson-like state in animals [66]. Being a highly lipophilic molecule, MPTP can successfully cross the BBB and auto-oxidize to MPP+. Within 12 to 72 hours, MPP+ can lower striatal dopamine levels and cause single nucleotide polymorphisms dopamine neurons to die. As a result, it is possible to develop both a chronic PD model with a continuous low-dose injection and an acute PD model with a single high-dose injection. To create an animal model, we employed an acute model of MPTP, which suppresses the mitochondrial complex that includes most of the clinical hallmarks of PD and amplifies oxidative stress and neuroinflammation [67].

To better understand the connection between neuronal degradation, recovery mechanisms, and the accompanying behavioral abnormalities, it is especially interesting to examine the behavioral deficits in MPTP model of PD [68]. According to a study, numerous tests, including locomotor activity, pole, cylinder, Y-maze, forced swim and open-field tests can be used to evaluate key symptoms of PD [69]. In our study, the motor function test revealed that, in comparison to the mice in the control and CDCA-treated groups, the MPTP-treated animals required longer to turn down on a pole. Another study has demonstrated that abnormalities in working memory are caused by MPTP lesioning [70]. To investigate altered behavior and spatial working memory, a non-motor

behavioral test called the Y-maze test was used. The findings demonstrate that the MPTP-treated mice's percentage of alternations, a measure of working memory, was considerably lower than that of the control and CDCA-treated groups. This lower alternation rate indicates that MPTP treatment impacted the memory of mice, reflecting the cognitive deficits associated with PD. On the other hand, a greater percentage of alternations was seen in the CDCA-treated group, suggesting an improvement in memory function.

PD shows a variety of locomotor dysfunction symptoms, such as rigidity, tremors, and bradykinesia [71]. Behavioral analysis reveals that CDCA enhanced locomotion and anxiety-like behavior as the results demonstrates that the diseased mice in this study spent more time in the peripheral and less time in the central region, suggesting increased anxiety and decreased exploratory behavior due to MPTP exposure. On the other hand, the CDCA-treated group behaved more like the control group, indicating that the treatment was successful in lowering anxiety and enhancing motor performance. One of the most common psychological symptoms is depression, which has been shown to begin before the onset of motor symptoms in PD [72]. Through the forced swim test and tail suspension, we were able to identify the antidepressant effects of CDCA as it decreased the immobility time and hence alleviated the depressive behavior in mice treated with MPTP. This behavioral data provides compelling evidence that CDCA improves motor impairment in PD mice, suggesting that it has beneficial impacts on neurological functions and improvement. It also successfully mitigated memory impairment and effectively alleviated depressive and anxiety like behavior, emphasizing its potential therapeutic benefits for cognitive function and depressive symptoms.

One of PD's neuropathological characteristics is the degeneration of dopamine neurons in the substantia nigra of the midbrain. As soon as clinical motor symptoms arise, 50–70% of dopamine neurons in the substantia nigra die and 70% of dopamine responsiveness disappears. It has been shown that systemic treatment of MPTP causes long-term cell death of nigrostriatal dopamine neurons and short-term dopamine depletion, resulting in selective neurodegeneration [73]. In our investigation, we discovered that when midbrain was exposed to MPTP, the cells suffered damage, changed shape, and decreased in number. On the other hand, by clearly increasing the number of neurons, CDCA therapy mitigated neurodegeneration in response to MPTP stimulation. A study has revealed that MPTP causes significant neuronal damage in hippocampus [74]. The reduction of neurons in the hippocampal region caused by MPTP was

considerably reduced by CDCA administration and this result is consistent with previous study [13]. Moreover, it has been proven that MPTP causes neurotoxicity to Purkinje cells in cerebellum of mice [75] which was also seen in our study and that neurotoxicity was reversed by CDCA by restoring the morphology of Purkinje cells.

Dopaminergic neuron loss in the nigro-striatal axis is the main focus of PD research [76]. However, the disorder also affects other parts of the brain, and relatively few studies have investigated the evolution of PD damage in areas like the cerebral cortex which is crucial to address the development of new and more effective therapeutic options [77]. Accordingly, a study that examined the neurotoxic effects of MPTP and neuroprotective effects of TUDCA in the cerebral cortex discovered that this PD model also affects the cerebral cortex [78]. Building on this discovery, we conducted more research on the cortex and found that MPTP intoxication caused a considerable loss of neurons as well as morphological degeneration. On the other hand, treatment with CDCA improved quantity and morphology of cortical neurons, indicating possible neuroprotective benefits and cortical function restoration. All of these findings revealed that CDCA efficiently improved neurodegeneration while also exhibiting positive neuroprotective effects in the brain.

It is commonly known that neurotrophic support is necessary for the development and survival of neurons, and that several variables are altered in PD, ultimately leading to excessive damage to dopaminergic neurons. The decrease of neurotrophic factors such as BDNF is one of the significant alterations. Dopaminergic neurons depend on neurotrophic factors to survive and operate properly. Since BDNF is highly expressed in dopaminergic neurons and is crucial to their survival, a decrease in it may result in both poor function and even the death of the cells [79]. Studies have confirmed that mice treated with MPTP had a significant drop in BDNF levels [80]. Another research has revealed that bile acids have the ability to operate as neurotrophic agents since they can activate nuclear receptors like the FXR as well as certain receptors like TGR5. The regulation of inflammation and apoptosis can be done by these receptors and hence they can indirectly increase the production and activity of BDNF [6]. In light of these investigations, we also looked at BDNF expression in our study and found that CDCA increased BDNF levels, which were considerably lower in the MPTP-treated mice. This implies that the use of CDCA may have encouraged neuronal regeneration in addition to protecting the dopaminergic neurons. These

results highlight the neuroprotective and neurogenic potential of CDCA, which may facilitate enhanced neuronal plasticity and functional recovery in PD.

It is widely recognized that Lewy bodies, a hallmark of PD, are created when α-synuclein misfolds and aggregates. Neurodegeneration and motor dysfunctions are linked to α-synuclein phosphorylation and accumulation in MPTP-treated mice [81, 82]. The expression of α-synuclein has been demonstrated to rise in MPTP intoxication [83]. Nevertheless, thioredoxin-1 overexpression inhibited rise in α-syn expression, whereas Trx-1 knockdown exacerbates it [84]. Furthermore, in MPTP-treated mice, lithium therapy was able to reduce the rise in α-synuclein expression in the substantia nigra region [85]. Our findings, which are in line with earlier investigations, demonstrated that MPTP-treated animals had significantly higher α-synuclein levels, indicating neurotoxicity. Interestingly, α-synuclein expression was markedly increased by CDCA therapy, indicating a possible neuroprotective impact. This improvement might be explained by CDCA's capacity to promote neuronal survival and regulate neuroinflammatory pathways, offering a potentially effective treatment for PD. Hence, the results strongly suggest that CDCA has a direct neuroprotective impact as the dopaminergic neurons were protected and motor impairments were lessened. Furthermore, decreased α-synuclein mRNA levels and notable rise in BDNF levels in PD model confirmed its neuroprotective and neurotrophic potential.

Limitations

1. There are several restrictions on our investigation. First, in PD models generated by MPTP, neuronal death is mediated by various pathways. Thus, additional signaling pathways may be involved in the neuroprotection mediated by CDCA. So, the molecular processes underlying CDCA's capacity for neuroprotection require more investigation.

2. Secondly, it is also essential to look at how CDCA affects neuroinflammatory processes as these mechanisms are acknowledged as important aspects of the pathology of PD.

3. Furthermore, none of the PD models can accurately replicate the pathophysiology and symptoms as seen in PD patients. The rapid degeneration of dopaminergic and other neurons in PD patients is probably not the same as the acute cell death progression shown in the MPTP-induced PD model. It is yet unknown what impact CDCA will have on PD clinically.

CHAPTER 5: SUMMARY OF RESEARCH WORK

In this work, we used an MPTP-induced mouse model of PD to examine the neuroprotective properties of CDCA. α--synuclein aggregation and the gradual degradation of dopaminergic neurons are the hallmarks of PD. In order to tackle these pathogenic characteristics, we used molecular docking studies to investigate CDCA's interactions with α-synuclein and BDNF. With binding energies ranging from -5.7 to -6.9 kcal/mol for BDNF and -4.6 to -5.3 kcal/mol for α-synuclein, the data showed that CDCA had substantial binding affinities with both substances, indicating possible neuroprotective processes. Behavioral evaluations, such as the pole test, demonstrated that in MPTP-treated mice, CDCA therapy markedly enhanced motor coordination and decreased bradykinesia. In addition, mice in the CDCA-treated group significantly improved on a number of behavioral tests, such as the forced swim test, open field test, Y-maze, and tail suspension test. These enhancements show that CDCA is an effective treatment for the behavioral abnormalities linked to PD.

In comparison to controls, histological examination with H&E staining revealed less neuronal loss in important brain regions of CDCA-treated animals. According to these results, CDCA interacts with BDNF to increase its neuroprotective effects, and it may block aggregation to lessen neurodegeneration when it interacts with α-synuclein. Moreover, the RT-PCR data show that the PD model has a significant increase in BDNF levels and a drop in α-synuclein mRNA levels, confirming the protein's neurotrophic and neuroprotective properties. Overall, this work sheds fresh light on the mechanisms of action and preclinical model efficacy of CDCA, highlighting its potential as a treatment agent for PD. To confirm these results and investigate the long-term impacts and safety profile of CDCA in clinical settings, more investigation is required.

CHAPTER 6: CONCLUSION AND FUTURE RECOMMENDATIONS

Effective anti-Parkinson's treatment may rely on both lowering neuronal degeneration and improving neuronal dysfunction, and our research targets both elements. Our research shows that MPTP-induced toxicity dramatically raises α-synuclein levels and damages mice's neuronal function, specifically impacting the cerebellum, hippocampus, cortex, and midbrain However, CDCA treatment effectively mitigates these effects, improving both α-synuclein and BDNF expression, as well as reducing neurodegeneration and restoring behavioral functions. Therefore, CDCA may have neurotrophic potential in addition to neuroprotective effects. Nonetheless, this research offers fresh insights into the possible therapeutic application of CDCA in the management of PD.

Future Recommendations

1. More research might examine the mechanisms by which CDCA affects the levels of BDNF and α-synuclein, offering more understanding of the pathophysiology and management of disease.

2. Future studies' primary objective might be to identify additional biomarkers associated with CDCA-induced neuroprotection. These biomarkers may aid in the early detection and monitoring of PD and other neurodegenerative diseases.

3. The non-motor symptoms that are commonly experienced by PD patients have a significant effect on their quality of life. Future research might investigate how CDCA-based neuroprotection affects these non-motor symptoms.

4. Using the results of our investigation to other neurodegenerative conditions including Lewy body dementia and Huntington's disease where BDNF and α-synuclein are involved.

5. Employing cutting-edge cellular models to investigate the effects of CDCA at the cellular and molecular levels, such as pluripotent stem cells obtained from individuals suffering from PD.

6. Using modern tools, including gene editing with CRISPR-Cas9 or modern imaging methods, to follow changes in neurons in vivo and explore the molecular impacts of CDCA.

7. Investigating the potential effects of lifestyle, nutrition, and environmental factors on the efficacy of CDCA treatment, ultimately leading to better management strategies of PD.

REFERENCES

1. Kaur, K. K., G. N. Allahbadia, and M. Singh. "An Update on Role of Bile Acids in Neurological Functions and Neurodegenerative Diseases: A Narrative Review." *J Clin Biomed Invest* 3.2 (2023): 22-39.

2. Kiriyama, Y., & Nochi, H. (2019). The biosynthesis, signaling, and neurological functions of bile acids. *Biomolecules*, *9*(6), 232.

3. Russell, D. W. (2003). The enzymes, regulation, and genetics of bile acid synthesis. *Annual review of biochemistry*, *72*(1), 137-174.

4. Ferdinandusse, S., & Houten, S. M. (2006). Peroxisomes and bile acid biosynthesis. *Biochimica et Biophysica Acta (BBA)-Molecular Cell Research*, *1763*(12), 1427-1440.

5. Grant, S. M., & DeMorrow, S. (2020). Bile acid signaling in neurodegenerative and neurological disorders. *International Journal of Molecular Sciences*, *21*(17), 5982.

6. Ackerman, H. D., & Gerhard, G. S. (2016). Bile acids in neurodegenerative disorders. *Frontiers in aging neuroscience*, *8*, 263.

7. Khalaf, K., Tornese, P., Cocco, A., & Albanese, A. (2022). Tauroursodeoxycholic acid: a potential therapeutic tool in neurodegenerative diseases. *Translational Neurodegeneration*, *11*(1), 33.

8. Cortez, L. M., Campeau, J., Norman, G., Kalayil, M., Van der Merwe, J., McKenzie, D., & Sim, V. L. (2015). Bile acids reduce prion conversion, reduce neuronal loss, and prolong male survival in models of prion disease. *Journal of virology*, *89*(15), 7660-7672.

9. Kiriyama, Y., & Nochi, H. (2023). Role of microbiota-modified bile acids in the regulation of intracellular organelles and neurodegenerative diseases. *Genes*, *14*(4), 825.

10. Elia, A. E., Lalli, S., Monsurrò, M. R., Sagnelli, A., Taiello, A. C., Reggiori, B., ... & Albanese, A. (2016). Tauroursodeoxycholic acid in the treatment of patients with amyotrophic lateral sclerosis. *European journal of neurology*, *23*(1), 45-52.

11. Chiang, J. Y., & Ferrell, J. M. (2018). Bile acid metabolism in liver pathobiology. *Gene expression*, *18*(2), 71.

12. Li, T., & Chiang, J. Y. (2014). Bile acid signaling in metabolic disease and drug therapy. *Pharmacological reviews*, *66*(4), 948-983.

13. Bazzari, F. H., Abdallah, D. M., & El-Abhar, H. S. (2019). Chenodeoxycholic acid ameliorates AlCl3-induced Alzheimer's disease neurotoxicity and cognitive deterioration via enhanced insulin signaling in rats. *Molecules*, *24*(10), 1992.

14. Koyama, S., Sekijima, Y., Ogura, M., Hori, M., Matsuki, K., Miida, T., & Harada-Shiba, M. (2021). Cerebrotendinous xanthomatosis: molecular pathogenesis, clinical spectrum, diagnosis, and disease-modifying treatments. *Journal of Atherosclerosis and Thrombosis*, *28*(9), 905-925.

15. Mou, Y., Nandi, G., Mukte, S., Chai, E., Chen, Z., Nielsen, J. E., ... & Li, X. J. (2023). Chenodeoxycholic acid rescues axonal degeneration in induced pluripotent stem cell-derived neurons from spastic paraplegia type 5 and cerebrotendinous xanthomatosis patients. *Orphanet Journal of Rare Diseases*, *18*(1), 72.

16. Nie, K., Li, Y., Zhang, J., Gao, Y., Qiu, Y., Gan, R., ... & Wang, L. (2022). Distinct Bile Acid Signature in Parkinson's Disease with Mild Cognitive Impairment. *Frontiers in neurology*, *13*, 897867.

17. Thomas, B., & Beal, M. F. (2007). Parkinson's disease. *Human molecular genetics*, *16*(R2), R183-R194.

18. Williams-Gray, C. H., & Worth, P. F. (2016). Parkinson's disease. *Medicine*, *44*(9), 542-546.

19. Schapira, A. H. (1999). Parkinson's disease. *Bmj*, *318*(7179), 311-314.

20. Naoi, M., & Maruyama, W. (1999). Cell death of dopamine neurons in aging and Parkinson's disease. *Mechanisms of ageing and development*, *111*(2-3), 175-188.

21. Guo, J. D., Zhao, X., Li, Y., Li, G. R., & Liu, X. L. (2018). Damage to dopaminergic neurons by oxidative stress in Parkinson's disease. *International journal of molecular medicine*, *41*(4), 1817-1825.

22. Mu, L., Chen, J., Sobotka, S., Nyirenda, T., Benson, B., Gupta, F., ... & Arizona Parkinson's Disease Consortium. (2015). Alpha-synuclein pathology in sensory nerve terminals of the upper aerodigestive tract of Parkinson's disease patients. *Dysphagia*, *30*, 404-417.

23. Schapira, A. H. (2006). Etiology of Parkinson's disease. *Neurology*, *66*(10_suppl_4), S10-S23.

24. Schapira, A. H., & Jenner, P. (2011). Etiology and pathogenesis of Parkinson's disease. *Movement disorders*, *26*(6), 1049-1055.

25. . Jonathan, Wistow. "Epidemiology." null (2022).:9-24. doi: 10.1093/med/9780190843014.003.0002.

26. Patil, R. R. (2022). Epidemiology of Parkinson's disease—current understanding of causation and risk factors. *Techniques for Assessment of Parkinsonism for Diagnosis and Rehabilitation*, 31-48.

27. Bock, M. A., & Tanner, C. M. (2022). The epidemiology of cognitive function in Parkinson's disease. *Progress in Brain Research*, *269*(1), 3-37.

28. Lees, A. J., Hardy, J., & Revesz, T. (2009). Parkinson's disease. *The Lancet*, *373*(9680), 2055-2066.

29. Bloem, B. R., Okun, M. S., & Klein, C. (2021). Parkinson's disease. *The Lancet*, *397*(10291), 2284-2303.

30. Samii, A., Nutt, J. G., & Ransom, B. R. (2004). Parkinson's disease. *The Lancet*, *363*(9423), 1783-1793.

31. Kalia, L. V., & Lang, A. E. (2015). Parkinson's disease. *The Lancet*, *386*(9996), 896-912.

32. Javier, B. L. E. S. A. (2012). Classic and New Animal Models of Parkinson's Disease. *Journal of Biomedicine and Biotechnology*, *845618*, 10.

33. Gubellini, P., & Kachidian, P. (2015). Animal models of Parkinson's disease: An updated overview. *Revue neurologique*, *171*(11), 750-761.

34. Konnova, E. A., & Swanberg, M. (2018). Animal models of Parkinson's disease. *Exon Publications*, 83-106.

35. Meredith, G. E., Sonsalla, P. K., & Chesselet, M. F. (2008). Animal models of Parkinson's disease progression. *Acta neuropathologica*, *115*, 385-398.

36. Meredith, G. E., & Rademacher, D. J. (2011). MPTP mouse models of Parkinson's disease: an update. *Journal of Parkinson's disease*, *1*(1), 19-33.

37. Mustapha, M., & Taib, C. N. M. (2021). MPTP-induced mouse model of Parkinson's disease: A promising direction for therapeutic strategies. *Bosnian journal of basic medical sciences*, *21*(4), 422.

38. Rizek, P., Kumar, N., & Jog, M. S. (2016). An update on the diagnosis and treatment of Parkinson disease. *Cmaj*, *188*(16), 1157-1165.

39. Savitt, J. M., Dawson, V. L., & Dawson, T. M. (2006). Diagnosis and treatment of Parkinson disease: molecules to medicine. *The Journal of clinical investigation*, *116*(7), 1744-1754.

40. Levine, C. B., Fahrbach, K. R., Siderowf, A. D., Estok, R. P., Ludensky, V. M., & Ross, S. D. (2003). Diagnosis and treatment of Parkinson's disease: a systematic review of the literature. *Evidence report/technology assessment (Summary)*, (57), 1-4.

41. Thaler, A., & Alcalay, R. N. (2022). Diagnosis and medical management of Parkinson disease. *CONTINUUM: Lifelong Learning in Neurology*, *28*(5), 1281-1300.

42. Singh, N., Pillay, V., & Choonara, Y. E. (2007). Advances in the treatment of Parkinson's disease. *Progress in neurobiology*, *81*(1), 29-44.

43. Stoker, T. B., & Barker, R. A. (2020). Recent developments in the treatment of Parkinson's Disease. *F1000Research*, *9*.

44. Ellis, J. M., & Fell, M. J. (2017). Current approaches to the treatment of Parkinson's Disease. *Bioorganic & medicinal chemistry letters*, *27*(18), 4247-4255.

45. Raghav, S., & Perju-Dumbrava, L. D. (2022). Treatment of Parkinson's Disease. *Techniques for Assessment of Parkinsonism for Diagnosis and Rehabilitation*, 105-117.

46. Wu, S. S., & Frucht, S. J. (2005). Treatment of Parkinson's disease: what's on the horizon?. *CNS drugs*, *19*, 723-743.

47. Dumbhare, O., & Gaurkar, S. S. (2023). A review of genetic and gene therapy for Parkinson's disease. *Cureus*, *15*(2).

48. Wal, A., Wal, P., Vig, H., Jain, N. K., Rathore, S., Krishnan, K., & Srivastava, A. (2023). Treatment of Parkinson's Disease: Current Treatments and Recent Therapeutic Developments. *Current Drug Discovery Technologies*, *20*(5), 54-70.

49. Waymouth-Wilson, A. C., Linklaw, B. J. P., Parker, G., Watts, J., Mortiboys, H., Bandmann, O., & Hastings, C. (2021). *2-fluorinated bile acids for the treatment of neurodegenerative diseases* (Patent No. CN113330020A). Chinese National Intellectual Property Administration. https://patents.google.com/patent/CN113330020A/en

50. Abdelkader, N. F. (2020). Ursodeoxycholic and tauroursodeoxycholic acids as antiapoptotic agents: modulation of Parkinson's disease. *Diagnosis and Management in Parkinson's Disease*, 653-664.

51. Can, A., Dao, D. T., Terrillion, C. E., Piantadosi, S. C., Bhat, S., & Gould, T. D. (2012). The tail suspension test. *JoVE (Journal of Visualized Experiments)*, (59), e3769.

52. Steru, L., Chermat, R., Thierry, B., & Simon, P. (1985). The tail suspension test: a new method for screening antidepressants in mice. *Psychopharmacology*, *85*, 367-370.

53. Seibenhener, M. L., & Wooten, M. C. (2015). Use of the open field maze to measure locomotor and anxiety-like behavior in mice. *JoVE (Journal of Visualized Experiments)*, (96), e52434.

54. Meredith, G. E., & Kang, U. J. (2006). Behavioral models of Parkinson's disease in rodents: a new look at an old problem. *Movement disorders*, *21*(10), 1595-1606.

55. Bogdanova, O. V., Kanekar, S., D'Anci, K. E., & Renshaw, P. F. (2013). Factors influencing behavior in the forced swim test. *Physiology & behavior*, *118*, 227-239.

56. Unal, G., & Canbeyli, R. (2019). Psychomotor retardation in depression: A critical measure of the forced swim test. *Behavioural brain research*, *372*, 112047.

57. Van der Borght, K., Havekes, R., Bos, T., Eggen, B. J., & Van der Zee, E. A. (2007). Exercise improves memory acquisition and retrieval in the Y-maze task: relationship with hippocampal neurogenesis. *Behavioral neuroscience*, *121*(2), 324.

58. Kumar, T. P., Antony, S., Soman, S., Kuruvilla, K. P., George, N., & Paulose, C. S. (2011). Role of curcumin in the prevention of cholinergic mediated cortical dysfunctions in streptozotocin-induced diabetic rats. *Molecular and cellular endocrinology*, *331*(1), 1-10.

59. Miedel, C. J., Patton, J. M., Miedel, A. N., Miedel, E. S., & Levenson, J. M. (2017). Assessment of spontaneous alternation, novel object recognition and limb clasping in transgenic mouse models of amyloid-β and tau neuropathology. *JoVE (Journal of Visualized Experiments)*, (123), e55523.

60. David, E. M., Pacharinsak, C., Jampachaisri, K., Hagan, L., & Marx, J. O. (2022). Use of ketamine or xylazine to provide balanced anesthesia with isoflurane in C57BL/6J mice. *Journal of the American Association for Laboratory Animal Science*, *61*(5), 457-467.

61. PFA

62. Binsuwaidan, R., Negm, W. A., Elekhnawy, E., Attallah, N. G., Ahmed, E., Magdeldin, S., ... & El-Sherbeni, S. A. (2023). In Vitro Antiviral Effect and Potential Neuroprotection of Salvadora persica L. Stem Bark Extract against Lipopolysaccharides-Induced Neuroinflammation in Mice: LC-ESI-MS/MS Analysis of the Methanol Extract. *Pharmaceuticals*, *16*(3), 398.

63. Hirsch, E. C., Hunot, S., & Hartmann, A. (2005). Neuroinflammatory processes in Parkinson's disease. *Parkinsonism & related disorders*, *11*, S9-S15.

64. Aminoff, M. J. (1994). Treatment of Parkinson's disease. *Western journal of medicine*, *161*(3), 303.

65. Cuevas, E., Burks, S., Raymick, J., Robinson, B., Gómez-Crisóstomo, N. P., Escudero-Lourdes, C., ... & Sarkar, S. (2022). Tauroursodeoxycholic acid (TUDCA) is neuroprotective in a chronic mouse model of Parkinson's disease. *Nutritional Neuroscience*, *25*(7), 1374-1391.

66. . Liu, W., Li, Y., Jalewa, J., Saunders-Wood, T., Li, L., & Hölscher, C. (2015). Neuroprotective effects of an oxyntomodulin analogue in the MPTP mouse model of Parkinson's disease. *European journal of pharmacology*, *765*, 284-290.

67. . Mao, Z., Hui, H., Zhao, X., Xu, L., Qi, Y., Yin, L., ... & Peng, J. (2023). Protective effects of dioscin against Parkinson's disease via regulating bile acid metabolism through remodeling gut microbiome/GLP-1 signaling. *Journal of Pharmaceutical Analysis*, *13*(10), 1153-1167.

68. Sedelis, M., Schwarting, R. K., & Huston, J. P. (2001). Behavioral phenotyping of the MPTP mouse model of Parkinson's disease. *Behavioural brain research*, *125*(1-2), 109-125.

69. Prasad, E. M., & Hung, S. Y. (2020). Behavioral tests in neurotoxin-induced animal models of Parkinson's disease. *Antioxidants*, *9*(10), 1007.

70. Ho, S. C., Hsu, C. C., Pawlak, C. R., Tikhonova, M. A., Lai, T. J., Amstislavskaya, T. G., & Ho, Y. J. (2014). Effects of ceftriaxone on the behavioral and neuronal changes in an MPTP-induced Parkinson's disease rat model. *Behavioural brain research*, *268*, 177-184.

71. Patil, S. P., Jain, P. D., Ghumatkar, P. J., Tambe, R., & Sathaye, S. (2014). Neuroprotective effect of metformin in MPTP-induced Parkinson's disease in mice. *Neuroscience*, *277*, 747-754.

72. Li, Y., Jiao, Q., Du, X., Bi, M., Han, S., Jiao, L., & Jiang, H. (2018). Investigation of behavioral dysfunctions induced by monoamine depletions in a mouse model of Parkinson's disease. *Frontiers in Cellular Neuroscience*, *12*, 241.

73. Li, H. Y., Liu, D. S., Li, L. B., Zhang, Y. B., Dong, H. Y., Rong, H., ... & Zhang, X. J. (2024). Total Glucosides of White Paeony Capsule ameliorates Parkinson's disease-like behavior in MPTP-induced mice model by regulating LRRK2/alpha-synuclein signaling. *Journal of Ethnopharmacology*, *319*, 117319.

74. Sriram, K., Matheson, J. M., Benkovic, S. A., Miller, D. B., Luster, M. I., & O'Callaghan, J. P. (2006). Deficiency of TNF receptors suppresses microglial activation and alters the susceptibility of brain regions to MPTP-induced neurotoxicity: role of TNF-α.

75. Takada, M., Sugimoto, T., & Hattori, T. (1993). MPTP neurotoxicity to cerebellar Purkinje cells in mice. *Neuroscience letters*, *150*(1), 49-52.

76. Poewe, W., Seppi, K., Tanner, C. M., Halliday, G. M., Brundin, P., Volkmann, J., ... & Lang, A. E. (2017). Parkinson disease. *Nature reviews Disease primers*, *3*(1), 1-21.

77. Becker, B., Demirbas, M., Johann, S., Zendedel, A., Beyer, C., Clusmann, H., ... & Kipp, M. (2018). Effect of intrastriatal 6-OHDA lesions on extrastriatal brain structures in the mouse. *Molecular neurobiology*, *55*, 4240-4252.

78. Mendes, M. O., Rosa, A. I., Carvalho, A. N., Nunes, M. J., Dionísio, P., Rodrigues, E., ... & Castro-Caldas, M. (2019). Neurotoxic effects of MPTP on mouse cerebral cortex: Modulation of neuroinflammation as a neuroprotective strategy. *Molecular and Cellular Neuroscience*, *96*, 1-9.

79. Haeri, P., Mohammadipour, A., Heidari, Z., & Ebrahimzadeh-Bideskan, A. (2019). Neuroprotective effect of crocin on substantia nigra in MPTP-induced Parkinson's disease model of mice. *Anatomical science international*, *94*, 119-127.

80. Xu, X. J., Pan, T., Fan, H. J., Wang, X., Yu, J. Z., Zhang, H. F., ... & Chai, Z. (2023). Neuroprotective effect of hyperoside in MPP+/MPTP-induced dopaminergic neurodegeneration. *Metabolic Brain Disease*, *38*(3), 1035-1050.

81. Gómez-Benito, M., Granado, N., García-Sanz, P., Michel, A., Dumoulin, M., & Moratalla, R. (2020). Modeling Parkinson's disease with the alpha-synuclein protein. *Frontiers in pharmacology*, *11*, 356.

82. . Hu, S., Hu, M., Liu, J., Zhang, B., Zhang, Z., Zhou, F. H., Wang, L., & Dong, J. (2020). Phosphorylation of Tau and α-Synuclein Induced Neurodegeneration in MPTP Mouse Model of Parkinson's Disease. *Neuropsychiatric disease and treatment*, *16*, 651–663.

83. Mani, S., Sekar, S., Barathidasan, R., Manivasagam, T., Thenmozhi, A. J., Sevanan, M., ... & Sakharkar, M. K. (2018). Naringenin decreases α-synuclein expression and neuroinflammation in MPTP-induced Parkinson's disease model in mice. *Neurotoxicity Research*, *33*, 656-670.

84. Gu, R., Bai, L., Yan, F., Zhang, S., Zhang, X., Deng, R., ... & Bai, J. (2024). Thioredoxin-1 decreases alpha-synuclein induced by MPTP through promoting autophagy-lysosome pathway. *Cell Death Discovery*, *10*(1), 93.

85. Zhao, Q., Liu, H., Cheng, J., Zhu, Y., Xiao, Q., Bai, Y., & Tao, J. (2019). Neuroprotective effects of lithium on a chronic MPTP mouse model of Parkinson's disease via regulation of α-synuclein methylation. *Molecular medicine reports*, *19*(6), 4989-4997.